arXiv:math/0611483v1 [math.AP] 15 Nov 2006

Spectra of Linearized Operators for NLS Solitary Waves

Shu-Ming Chang[*] Stephen Gustafson[†] Kenji Nakanishi[‡] Tai-Peng Tsai[§]

Abstract. Nonlinear Schrödinger (NLS) equations with focusing power nonlinearities have solitary wave solutions. The spectra of the linearized operators around these solitary waves are intimately connected to stability properties of the solitary waves, and to the long-time dynamics of solutions of (NLS). We study these spectra in detail, both analytically and numerically.

Key words. Spectrum, linearized operator, NLS, solitary waves, stability.

AMS subject classifications. 35Q55, 35P15.

1 Introduction

Consider the nonlinear Schrödinger equation (NLS) with focusing power nonlinearity,

$$i\partial_t\psi = -\Delta\psi - |\psi|^{p-1}\psi, \tag{1.1}$$

where $\psi(t,x) : \mathbb{R}\times\mathbb{R}^n \to \mathbb{C}$ and $1 < p < \infty$. Such equations arise in many physical settings, including nonlinear optics, water waves, and quantum physics. Mathematically, nonlinear Schrödinger equations with various nonlinearities are studied as basic models of nonlinear dispersive phenomena. In this paper, we stick to the case of a pure power nonlinearity for the sake of simplicity.

For a certain range of the power p (see below), the NLS (1.1) has special solutions, of the form $\psi(t,x) = Q(x)\,e^{it}$. These are called *solitary waves*. The aim of this paper is to study the spectra of the *linearized operators* which arise when (1.1) is linearized around solitary waves. The main motivation for this study is that properties of these spectra are intimately related to the problem of the stability (orbital and asymptotic) of these solitary waves, and to the long-time dynamics of solutions of NLS.

Let us begin by recalling some well-known facts about (1.1). Standard references include [4, 33, 34]. Many basic results on the linearized operators we study here were proved by

[*]Department of Mathematics, National Tsing Hua University, Hsinchu, Taiwan (schang@mx.nthu.edu.tw)

[†]Department of Mathematics, University of British Columbia, Vancouver, BC V6T1Z2, Canada (gustaf@math.ubc.ca)

[‡]Department of Mathematics, Kyoto University, Kyoto 606-8502, Japan (n-kenji@math.kyoto-u.ac.jp)

[§]Department of Mathematics, University of British Columbia, Vancouver, BC V6T1Z2, Canada (ttsai@math.ubc.ca)

Weinstein [38, 39]. The Cauchy (initial value) problem for equation (1.1) is locally (in time) well-posed in $H^1(\mathbb{R}^n)$ if $1 < p < p_{\max}$, where

$$p_{\max} := 1 + 4/(n-2) \quad \text{if } n \geq 3; \quad p_{\max} := \infty \quad \text{if } n = 1, 2.$$

Moreover, if $1 < p < p_c$ where

$$p_c := 1 + 4/n,$$

the problem is globally well-posed. For $p \geq p_c$, there exist solutions whose H^1-norms go to ∞ (*blow up*) in finite time. In this paper, the cases $p < p_c$, $p = p_c$ and $p > p_c$ are called *sub-critical*, *critical*, and *super-critical*, respectively.

The set of all solutions of (1.1) is invariant under the symmetries of translation, rotation, phase, Galilean transform and scaling: if $\psi(t, x)$ is a solution, then so is

$$\widetilde{\psi}(t, x) := \lambda^{2/(p-1)} \psi\left(\lambda^2 t,\ \lambda R x - \lambda^2 t v - x_0\right) \exp\left\{ i \left[\frac{\lambda R x \cdot v}{2} - \frac{\lambda^2 t v^2}{4} + \gamma_0 \right] \right\}$$

for any constant $x_0, v \in \mathbb{R}^n$, $\lambda > 0$, $\gamma_0 \in \mathbb{R}$ and $R \in O(n)$. When $p = p_c$, there is an additional symmetry called the "pseudo-conformal transform" (see [34, p.35]).

We are interested here in solutions of (1.1) of the form

$$\psi(t, x) = Q(x)\, e^{it} \tag{1.2}$$

where $Q(x)$ must therefore satisfy the nonlinear elliptic equation

$$-\Delta Q - |Q|^{p-1} Q = -Q. \tag{1.3}$$

Any such solution generates a family of solutions by the above-mentioned symmetries, called *solitary waves*. Solitary waves are special examples of *nonlinear bound states*, which, roughly speaking, are solutions that are spatially localized for all time. More precisely, one could define nonlinear bound states to be solutions $\psi(t, x)$ which are *non-dispersive* in the sense that

$$\sup_{t \in \mathbb{R}} \inf_{x_0 \in \mathbb{R}^n} \| |x| \psi(t, x - x_0) \|_{L^2_x(\mathbb{R}^n)} < \infty.$$

Testing (1.3) with $\bar{Q}$ and $x.\nabla \bar{Q}$ and taking real parts, one arrives at the *Pohozaev identity* ([27])

$$\frac{1}{2} \int |Q|^2 = b \frac{1}{p+1} \int |Q|^{p+1}, \quad \frac{1}{2} \int |\nabla Q|^2 = a \frac{1}{p+1} \int |Q|^{p+1} \tag{1.4}$$

where

$$a = \frac{n(p-1)}{4}, \quad b = \frac{n + 2 - (n-2)p}{4}.$$

The coefficients a and b must be positive, and hence a necessary condition for existence of non-trivial solutions is $p \in (1, p_{\max})$.

For $p \in (1, p_{\max})$, and for all space dimensions, there exists at least one non-trivial radial solution $Q(x) = Q(|x|)$ of (1.3) (existence goes back to [27]). This solution, called a *nonlinear ground state*, is smooth, decreases monotonically as a function of $|x|$, decays exponentially at infinity, and can be taken to be positive: $Q(x) > 0$. It is the unique positive solution. (See [34] for references for the various existence and uniqueness results for various nonlinearities.) The ground state can be obtained as the minimizer of several different variational problems. One such result we shall briefly use later is that, for all $n \geq 1$ and $p \in (1, p_{\max})$, the ground state minimizes the Gagliardo-Nirenberg quotient

$$J[u] := \frac{\left(\int |\nabla u|^2\right)^a \left(\int u^2\right)^b}{\int u^{p+1}} \tag{1.5}$$

among nonzero $H^1(\mathbb{R}^n)$ radial functions (Weinstein [38]).

For $n = 1$, the ground state is the unique $H^1(\mathbb{R})$-solution of (1.3) up to translation and phase [4, p.259, Theorem 8.1.6]. For $n \geq 2$, this is not the case: there are countably infinitely many radial solutions (still real-valued), denoted in this paper by $Q_{0,k,p}(x)$, $k = 0, 1, 2, 3, \ldots$, each with exactly k positive zeros as a function of $|x|$ (Strauss [32]; see also [2]). In this notation, $Q_{0,0,p}$ is the ground state.

There are also non-radial (and complex-valued) solutions, for example those suggested by P. L. Lions [20] with non-zero angular momenta,

$$n = 2, \quad Q = \phi(r)\, e^{im\theta}, \qquad \text{in polar coordinates } r, \theta;$$

$$n = 3, \quad Q = \phi(r, x_3)\, e^{im\theta}, \qquad \text{in cylindrical coordinates } r, \theta, x_3,$$

and similarly defined for $n \geq 4$. When $n = 2$, some of these solutions are denoted here by $Q_{m,k,p}$ with $p \in (1, p_{\max})$ and $k = 0, 1, 2, \ldots$ denoting their numbers of positive zeros. See Section 4 for more details.

We will refer to all the solitary waves generated by $Q_{0,0,p}$ as *nonlinear ground states*, and all others as *nonlinear excited states*. We are not aware of a complete characterization of all solutions of (1.3), or of (1.1). For example, the uniqueness of $Q_{m,k,p}$ with $m, k \geq 1$ is apparently open. Also, we do not know if there are "breather" solutions, analogous to those of the generalized KdV equations. In this paper we will mainly study radial solutions (and in particular the ground state), but we will also briefly consider non-radial solutions numerically in Section 4.

To study the stability of a solitary wave solution (1.2), one considers solutions of (NLS) of the form

$$\psi(t, x) = [Q(x) + h(t, x)]\, e^{it}. \tag{1.6}$$

For simplicity, let $Q = Q_{0,0,p}$ be the ground state for the remainder of this introduction (see Section 4 for the general case). The perturbation $h(t, x)$ satisfies an equation

$$\partial_t h = \mathcal{L}h + (\text{nonlinear terms}) \tag{1.7}$$

where $\mathcal{L}$ is the *linearized operator* around Q:

$$\mathcal{L}h = -i\left\{(-\Delta + 1 - Q^{p-1})h - \tfrac{p-1}{2}\,Q^{p-1}(h+\bar{h})\right\}. \tag{1.8}$$

It is convenient to write $\mathcal{L}$ as a matrix operator acting on $\begin{bmatrix}\operatorname{Re} h\\ \operatorname{Im} h\end{bmatrix}$,

$$\mathcal{L} = \begin{bmatrix} 0 & L_- \\ -L_+ & 0 \end{bmatrix} \tag{1.9}$$

where

$$L_+ = -\Delta + 1 - pQ^{p-1}, \qquad L_- = -\Delta + 1 - Q^{p-1}. \tag{1.10}$$

Clearly the operators L_- and L_+ play a central role in the stability theory. They are self-adjoint Schrödinger operators with continuous spectrum $[1,\infty)$, and with finitely many eigenvalues below 1. In fact, when Q is the ground state, it is easy to see that L_- is a nonnegative operator, while L_+ has exactly one negative eigenvalue (these facts follow from Lemma 2.2 below).

Because of its connection to the stability problem, the object of interest to us in this paper is the spectrum of the non-self-adjoint operator $\mathcal{L}$. The simplest properties of this spectrum are

1. for all $p \in (1, p_{\max})$, 0 is an eigenvalue of $\mathcal{L}$.
2. the set $\Sigma_c := \{ir : r \in \mathbb{R}, |r| \geq 1\}$ is the continuous spectrum of $\mathcal{L}$.

(See the next section for the first statement. The second is easily checked.)

It is well-known that the exponent $p = p_c$ is critical for stability of the ground state solitary wave (as well as for blow-up of solutions). For $p < p_c$ the ground state is *orbitally stable*, while for $p \geq p_c$ it is unstable (see [40, 12]). These facts have immediate spectral counterparts: for $p \in (1, p_c]$, all eigenvalues of $\mathcal{L}$ are purely imaginary, while for $p \in (p_c, p_{\max})$, $\mathcal{L}$ has at least one eigenvalue with positive real part.

The goal of this paper is to get a more detailed understanding of the spectrum of $\mathcal{L}$, using both analytical and numerical techniques. See [11, 6, 7, 8] for related work. This finer information is essential for understanding the long-time dynamics of solutions of (NLS), for example: (i) to prove asymptotic (rather than simply orbital) stability, one often assumes either the linearized operator $\mathcal{L}$ has no nonzero eigenvalue, or its nonzero eigenvalues are $\pm ri$ with $0.5 < r < 1$. These assumptions need to be verified; (ii) to determine the rate of relaxation to stable solitary waves when there is a unique pair of nonzero eigenvalues $\pm ri$ with $0 < r < 1$. Heuristic arguments suggest that $[1/r]$, the smallest integer no longer that $1/r$, may decide the rate; (iii) to construct stable manifolds of unstable solitary waves, one needs to know if there are eigenvalues which are not purely imaginary, and to find their locations. These are highly active areas of current research, see e.g. [13, 17, 31] and the references therein.

Interesting questions with direct relevance to these stability-type problems include:

(i) Can one determine (or estimate) the number and locations of the eigenvalues of $\mathcal{L}$ lying on the segment between 0 and i?

(ii) Can $\pm i$, the thresholds of the continuous spectrum Σ_c, be eigenvalues or resonances?

(iii) Can eigenvalues be embedded inside the continuous spectrum?

(iv) Can the linearized operator have eigenvalues with non-zero real *and* imaginary parts (this is already known not to happen for the ground state – see the next section – and so we pose this question with excited states in mind).

(v) Are there bifurcations, as p varies, of pairs of purely imaginary eigenvalues into pairs of eigenvalues with non-zero real part (a stability/instability transition)?

The detailed discussion of the numerical methods is postponed to the Appendix. Roughly speaking, we first compute the nonlinear ground state by iteration and renormalization, and then compute the spectra of various suitably discretized linear operators.

Let us now summarize the main results and observations of this paper.

1. **Numerics for spectra.** When Q is the ground state, we compute numerically the spectra of $\mathcal{L}$, L_+ and L_- as functions of p, see Figures 1–5. In these figures, the horizontal axis is the logarithm of $p-1$. The vertical axis is: Solid lines are purely imaginary eigenvalues of $\mathcal{L}$ (without i) for $\in (1, p_c)$; dashed lines are real eigenvalues of $\mathcal{L}$; dotted line are eigenvalues of L_+; dashdot lines are eigenvalues of L_-. We have ignored imaginary eigenvalues of the discretized operators with modulus greater than one, which correspond to the continuous spectra of the original operators. Figure 1 is the one-dimensional case. Figures 2 and 3 are the spectra of these operators restricted to radial functions, for space dimensions $n = 2$ and 3. Figures 4 and 5 are for $n = 2$ and are the spectra restricted to functions of the form $\phi(r)e^{i\theta}$ and $\phi(r)e^{i2\theta}$, respectively. These pictures shed some light on questions (i), (iv), and (v) above, and to a certain extent on question (ii).

   Figures 10–15 are concerned with the spectra of excited states, see discussion below.

2. **One-dimensional phenomena.** The case $n = 1$ is the easiest case to handle analytically. In Section 3, we undertake a detailed study of the one-dimensional problem, giving rigorous proofs of a number of phenomena observed in Figure 1. One simple such phenomenon is the (actually classical) fact that the eigenvalues of L_+ and L_- exactly coincide, with the exception of the first, negative, eigenvalue of L_+ (note that this appears to be a strictly one-dimensional phenomenon: the eigenvalues of L_+ and L_- are different for $n \geq 2$, as Figures 2–5 indicate). In fact, we are able to prove sufficiently precise upper and lower bounds on the eigenvalues of $\mathcal{L}$ (lying outside the continuous spectrum) to determine their number, and estimate their positions, as functions of p (see Theorem 3.8). We use two basic techniques: an embedding of L_+ and L_- into a hierarchy of related operators, and a novel variational problem for

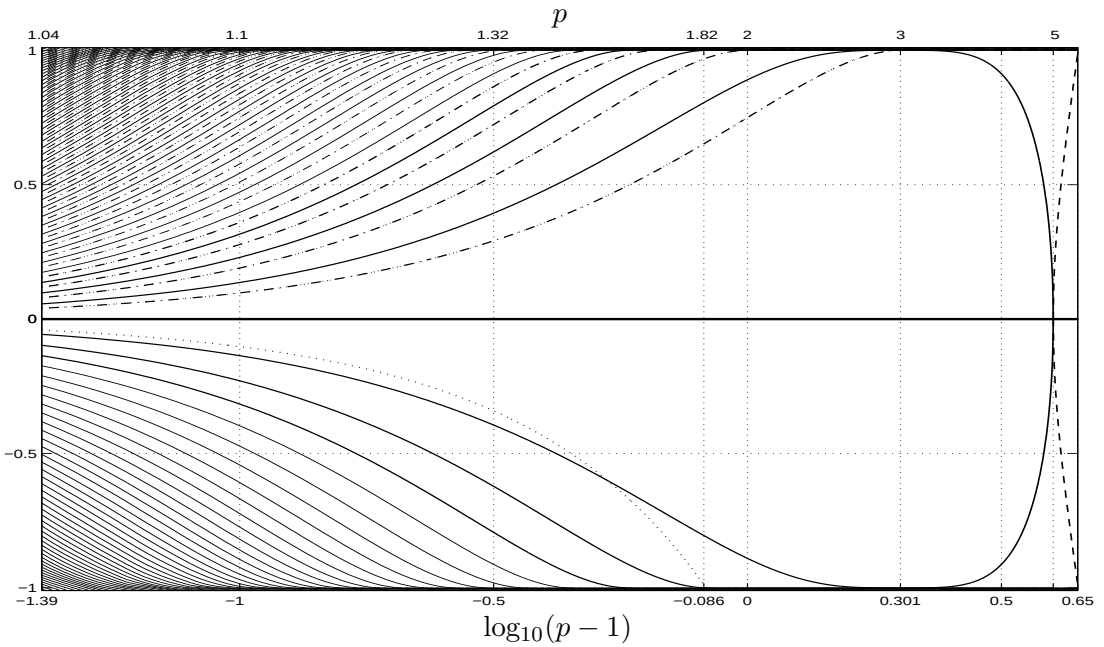

Figure 1: Spectra of $\mathcal{L}$, L_+ and L_- for $n = 1$ with logarithmic axis for the values of $p - 1$. (solid line: purely imaginary eigenvalues of $\mathcal{L}$; dashed line: real eigenvalues of $\mathcal{L}$; dotted line: eigenvalues of L_+; dashdot line: eigenvalues of L_-)

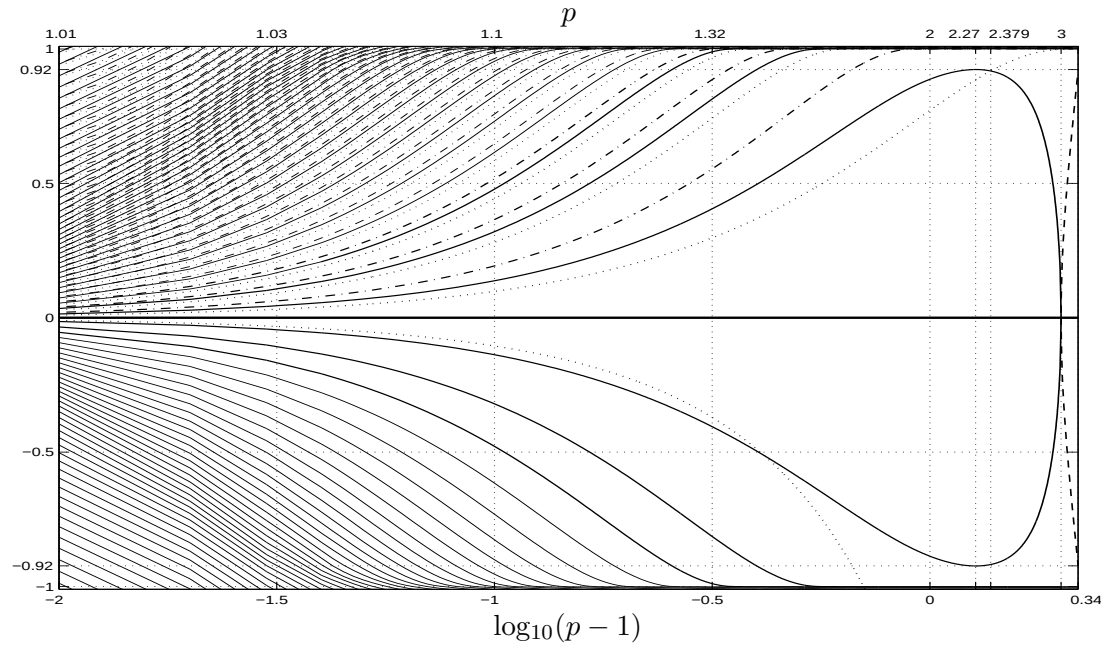

Figure 2: Spectra of $\mathcal{L}$, L_+ and L_- restricted to radial functions in the two-dimensional space, with logarithmic axis for the values of $p-1$. (solid line: purely imaginary eigenvalues of $\mathcal{L}$; dashed line: real eigenvalues of $\mathcal{L}$; dotted line: eigenvalues of L_+; dashdot line: eigenvalues of L_-)

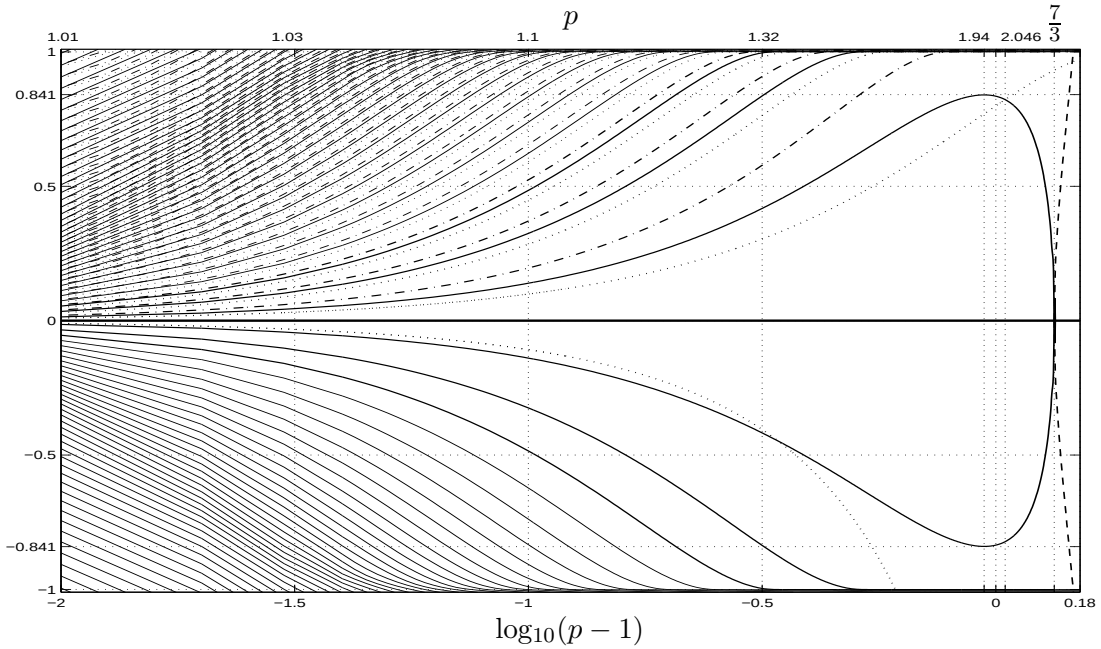

Figure 3: Spectra of $\mathcal{L}$, L_+ and L_- restricted to radial functions in the three-dimensional space.

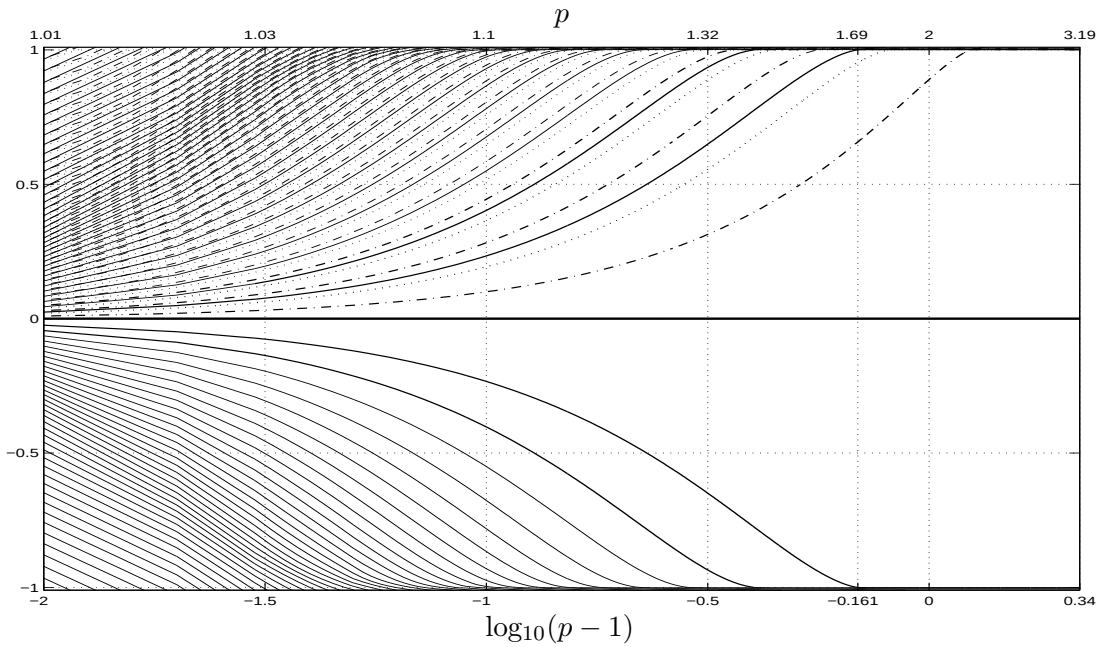

Figure 4: Spectra of $\mathcal{L}$, L_+ and L_- restricted to functions of the form $\phi(r)e^{i\theta}$ in the two-dimensional space.

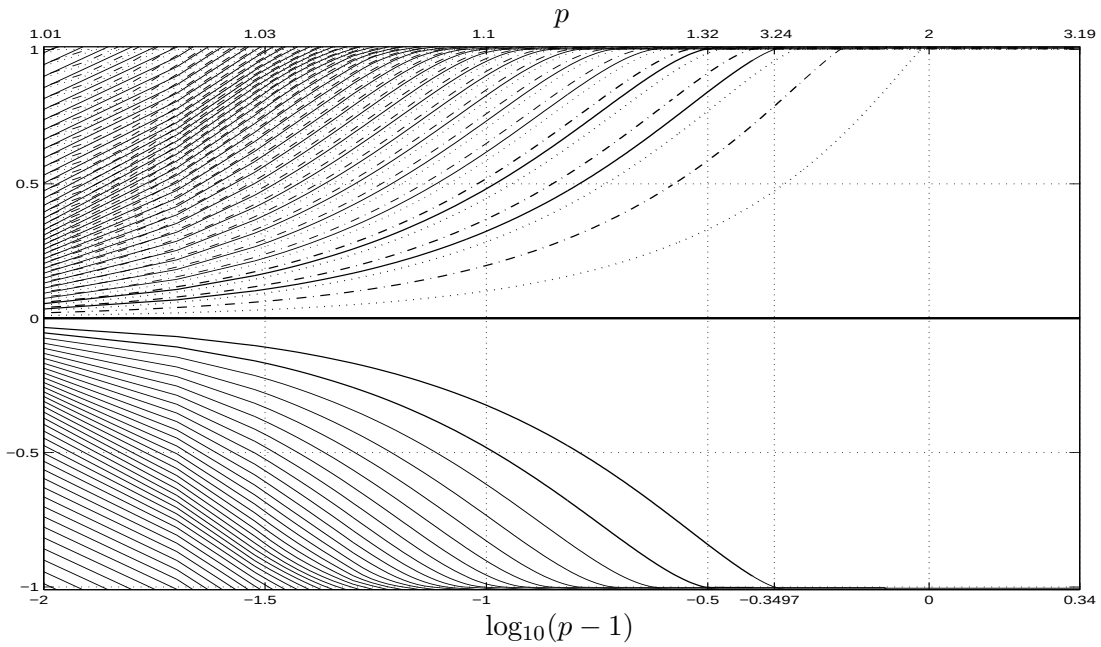

Figure 5: Spectra of $\mathcal{L}$, L_+ and L_- restricted to functions of the form $\phi(r)e^{i2\theta}$ in the two-dimensional space.

the eigenvalues, in terms of a 4-th order self-adjoint differential operator (see Theorem 3.6). In this way, we get a fairly complete answer to question (i) above for $n = 1$.

3. **Variational characterization of eigenvalues**. We present self-adjoint variational formulations of the eigenvalue problem for $\mathcal{L}$ in any dimension (see Summary 2.5), including the novel $n = 1$ formulation mentioned above. In principle, these provide a means of counting/estimating the eigenvalues of $\mathcal{L}$ (and hence addressing question (i) above in higher dimensions), though we only obtain detailed such information for $n = 1$.

4. **Bifurcation at $p = p_c$.** In each of Figures 1–3, a pair of purely imaginary eigenvalues for $p < p_c$ appears to collide at 0 at $p = p_c$, and become a pair of real eigenvalues for $p > p_c$. This is exactly the stability/instability transition for the ground state. We rigorously verify this picture, determining analytically the spectrum near 0 for p near p_c, and making concrete a bifurcation picture suggested by M. I. Weinstein (personal communication): see Theorem 2.6. This gives a partial answer to question (v) above. It is worth pointing out that for $n = 1$, the imaginary part of the (purely imaginary) eigenvalue bifurcating for $p < p_c$ is always larger than the third eigenvalue of L_+ (the first is negative and the second is zero) – this is proved analytically in Theorem 3.8. For $n \geq 2$, however, they intersect at $p \approx 2.379$ for 2D and $p \approx 2.046$ for 3D, (see Figures 1–3).

5. **Interlacing property.** A numerical observation: in all the figures, the adjacent eigenvalues of $\mathcal{L}$ seem each to bound an eigenvalue of L_+ and one of L_- (at least for p small enough). We are able to establish this "interlacing" property analytically in dimension one (see Theorem 3.8).

6. **Threshold resonance**. An interesting fact observed numerically (Figure 1) is that, in the 1D case, as $p \to 3$, one eigenvalue curve converges to $\pm i$, the threshold of the continuous spectrum. One might suspect that, at $p = 3$, $\pm i$ corresponds to a resonance or embedded eigenvalue. It is indeed a resonance: we find an explicit non spatially-decaying "eigenfunction", and show numerically in Section 3.7 that the corresponding eigenfunctions converges, as $p \to 3$, to this function. This observation addresses question (ii) above for $n = 1$.

7. **Excited states**. In Section 4 we consider the spectra of linearized operators around excited states with non-zero angular momenta. We observe that, in addition to the bifurcation mentioned above at $p = p_c$, there are complex eigenvalues which are neither real nor purely imaginary (addressing question (iv) above; see Figures 10–15), symmetric with respect to both real and purely imaginary axes. These complex eigenvalues also come from bifurcation: as p decreases, a quadruple of complex eigenvalues will collide into the imaginary axis away from 0, and then split to 4 purely imaginary eigenvalues. It seems that all eigenvalues lie on the imaginary axis for $p \in (1, p_*)$ for some p_* close to 1. In other words, *numerically these excited states are spectrally stable for p close to* 1. It is possible that the numerical error increases enormously as $p \to 1_+$ due to the artificial boundary condition, since the spectrum is approaching to the continuous one for $p = 1$. This has to be verified analytically in the future. Even if they are indeed spectrally stable, it is not clear if they are *nonlinearly* stable.

It is worth mentioning some important questions we *cannot* answer:

1. We are so far unable to give precise rigorous estimates on the number and positions of the eigenvalues of $\mathcal{L}$ for $n \geq 2$ (question (i) above).

2. We cannot exclude the possible existence of embedded eigenvalues (question (iii) above).

3. We do not know a nice variational formulation for eigenvalues of $\mathcal{L}$ when Q is an *excited* state (this problem is also linked to question (i) above).

4. We do not have a complete characterization of solitary waves, or more generally of nonlinear bound states.

We end this introduction by describing some related numerical work. Buslaev-Grikurov [3, 10] study the linearized operators for solitary waves of the following 1D NLS with $p < q$,

$$i\psi_t + \psi_{xx} + |\psi|^p\psi - \alpha|\psi|^q\psi = 0.$$

They draw the bifurcation picture for eigenvalues near zero when the parameter $\alpha > 0$ is near a critical value, with the frequency of the solitary wave fixed. This picture is similar to Weinstein's picture which we study in Section 2.3.

Demanet and Schlag [8] consider the same linearization as us and study the super-critical case $n = 3$ and $p \leq 3$ near 3. In this case, it is numerically shown that both L_+ and L_- have no eigenvalues in $(0, 1]$ and no resonance at 1, a condition which implies (see [31]) that $\mathcal{L}$ has no purely imaginary eigenvalues in $[-i, 0) \cup (0, i]$ and no resonance at $\pm i$.

We outline the rest of the paper: in Section 2 we consider general results for all dimensions for ground states. In Section 3 we consider one dimensional theory. In Section 4 we discuss the spectra for excited states with angular momenta. In the Appendix we discuss the numerical methods.

Notation: For an operator A, $N(A) = \left\{\phi \in L^2 |\ A\phi = 0\right\}$ denotes the nullspace of A. $N_g(A) = \cup_{k=1}^{\infty} N(A^k)$ denotes the generalized nullspace of A. The L^2-inner product in $\mathbb{R}^n$ is $(f, g) = \int_{\mathbb{R}^n} \bar{f} g \, dx$.

2 Revisiting the general theory for ground states

In this section we review mostly well-known results which are valid for all dimensions, for the ground state $Q(x) = Q_{0,0,p}(x)$, and give new proofs of some statements.

We begin by recalling some well-known results for the linearized operator $\mathcal{L}$ defined by (1.8). As is well known for linearized Hamiltonian system (and can be checked directly), if λ is an eigenvalue, then so are $-\lambda$ and $\pm\bar{\lambda}$. Hence if $\lambda \neq 0$ is real or purely imaginary, it comes in a pair. If it is complex with nonzero real and imaginary parts, it comes in a quadruple. It follows from nonlinear stability and instability results [40, 12] that all eigenvalues are purely imaginary if $p \in (1, p_c)$, and that there is at least one eigenvalue with positive real part when $p \in (p_c, p_{\max})$. It is also known (see e.g. [7]) that the set of isolated and embedded eigenvalues is finite, and the dimensions of the corresponding generalized eigenspaces are finite.

2.1 L_+, L_-, and the generalized nullspace of $\mathcal{L}$

Here we recall the makeup of the generalized nullspace $N_g(\mathcal{L})$ of $\mathcal{L}$. Easy computations give

$$L_+ Q_1 = -2Q, \quad L_- Q = 0, \quad \text{where } Q_1 := (\tfrac{2}{p-1} + x \cdot \nabla)Q, \tag{2.1}$$

and

$$L_- xQ = -2\nabla Q, \quad L_+ \nabla Q = 0. \tag{2.2}$$

In the critical case $p = p_c$, we also have

$$L_-(|x|^2 Q) = -4Q_1, \quad L_+ \rho = |x|^2 Q \tag{2.3}$$

for some radial function $\rho(x)$ (for which we do not know an explicit formula in terms of Q). Denote

$$\delta^p_{p_c} = \begin{cases} 1 & p = p_c \\ 0 & p \neq p_c. \end{cases} \tag{2.4}$$

For $1 < p < p_{max}$, the generalized nullspace of $\mathcal{L}$ is given by (see [39])

$$N_g(\mathcal{L}) = \text{span}\left\{ \begin{bmatrix} 0 \\ Q \end{bmatrix}, \begin{bmatrix} 0 \\ xQ \end{bmatrix}, \delta_{p_c}^p \begin{bmatrix} 0 \\ |x|^2 Q \end{bmatrix}, \begin{bmatrix} \nabla Q \\ 0 \end{bmatrix}, \begin{bmatrix} Q_1 \\ 0 \end{bmatrix}, \delta_{p_c}^p \begin{bmatrix} \rho \\ 0 \end{bmatrix} \right\}. \tag{2.5}$$

In particular

$$\dim N_g(\mathcal{L}) = 2n + 2 + 2\delta_{p_c}^p.$$

The fact that the vectors on the r.h.s of (2.5) lie in $N_g(\mathcal{L})$ follows immediately from the computations (2.1)-(2.3). That these vectors span $N_g(\mathcal{L})$ is established in [39], Theorems B.2 and B.3, which rely on the non-degeneracy of the kernel of L_+:

Lemma 2.1 *For all $n \geq 1$ and $p \in (1, p_{\max})$,*

$$N(L_+) = \text{span}\{\nabla Q\}$$

This lemma is proved in [39] for certain n and p ($n = 1$ and $1 < p < \infty$, or $n = 3$ and $1 < p \leq 3$), and is completely proved later by a general result of [18]. We present here a direct proof of this lemma, without referring to [18], relying only on oscillation properties of Sturm-Liouville ODE eigenvalue problems. A similar argument (which in the present case, however, applies only for $p \leq 3$) appears in [14], Appendix C. For completeness, we also include some arguments of [39].

A new proof. We begin with the cases $n \geq 2$. Since the potential in L_+ is radial, any solution of $L_+ v = 0$ can be decomposed as $v = \sum_{k \geq 0} \sum_{\mathbf{j} \in \Sigma_k} v_{k,\mathbf{j}}(r) Y_{k,\mathbf{j}}(\hat{x})$, where $r = |x|$, $\hat{x} = \frac{x}{r}$ is the spherical variable, and $Y_{k,\mathbf{j}}$ denote spherical harmonics: $-\Delta_{S^{n-1}} Y_{k,\mathbf{j}} = \lambda_k Y_{k,\mathbf{j}}$ (a secondary multi-index $\mathbf{j}$, appropriate to the dimension, runs over a finite set Σ_k for each k). Then $L_+ v = 0$ can be written as $A_k v_{k,\mathbf{j}} = 0$, where, for $k = 0, 1, 2, 3, \ldots$,

$$A_0 = -\partial_r^2 - \frac{n-1}{r}\partial_r + 1 - pQ^{p-1}(r), \quad A_k = A_0 + \lambda_k r^{-2}, \quad \lambda_k = k(k+n-2).$$

Case 1: $k = 1$. Note $\nabla Q = Q'(r)\hat{x}$. Since $A_1 Q' = 0$ and $Q'(r) < 0$ (monotonicity of the ground state) for $r \in (0, \infty)$, $Q'(r)$ is the unique ground state of A_1 (up to a factor), and so $A_1 \geq 0$, $A_1|_{\{Q'\}^\perp} > 0$.

Case 2: $k \geq 2$. Since $A_k = A_1 + (\lambda_k - \lambda_1) r^{-2}$ and $\lambda_k > \lambda_1$, we have $A_k > 0$, and hence $A_k v_k = 0$ has no nonzero L^2-solution.

Case 3: $k = 0$. Note that the first eigenvalue of A_0 is negative because $(Q, A_0 Q) = (Q, -(p-1)Q^p) < 0$. The second eigenvalue is non-negative due to (2.7) and the minimax principle. Hence, if there is a nonzero solution of $A_0 v_0 = 0$, then 0 is the second eigenvalue. By Sturm-Liouville theory, $v_0(r)$ can be taken to have only one positive zero, which we denote by $r_0 > 0$. By (2.1), $A_0 Q = -(p-1)Q^p$ and $A_0 Q_1 = -2Q$. Hence $(Q^p, v_0) = 0 = (Q, v_0)$. Let $\alpha = (Q(r_0))^{p-1}$. Since $Q'(r) < 0$ for $r > 0$, the function $Q^p - \alpha Q = Q(Q^{p-1} - \alpha)$ is positive for $r < r_0$ and negative for $r > r_0$. Thus $v_0(Q^p - \alpha Q)$ does not change sign, contradicting $(v_0, Q^p - \alpha Q) = 0$. Combining all these cases gives Lemma 2.1 for $n \geq 2$.

Finally, consider $n = 1$. Suppose $L_+ v = 0$. Since L_+ preserves oddness and evenness, we may assume v is either odd or even. If it is odd, it vanishes at the origin, and so by linear ODE uniqueness, v is a multiple of Q'. So suppose v is even. As in Case 3 above, since L_+ has precisely one negative eigenvalue, and has Q' in its kernel, $v(x)$ can be taken to have two zeros, at $x = \pm x_0$, $x_0 \neq 0$. The argument of Case 3 above then applies on $[0, \infty)$ to yield a contradiction. □

We complete this section by summarizing some positivity estimates for the operators L_+ and L_-. These estimates are closely related to the stability/instability of the ground state.

Lemma 2.2

$$L_- \geq 0, \quad L_-|_{\{Q\}^\perp} > 0 \quad (1 < p < p_{\max}) \tag{2.6}$$

$$(Q, L_+ Q) < 0, \quad L_+|_{\{Q^p\}^\perp} \geq 0 \quad (1 < p < p_{\max}), \tag{2.7}$$

$$L_+|_{\{Q\}^\perp} \geq 0 \quad (1 < p \leq p_c) \tag{2.8}$$

$$L_+|_{\{Q, xQ\}^\perp} > 0, \quad L_-|_{\{Q_1\}^\perp} > 0 \quad (1 < p < p_c) \tag{2.9}$$

$$L_+|_{\{Q, xQ, |x|^2 Q\}^\perp} > 0, \quad L_-|_{\{Q_1, \rho\}^\perp} > 0 \quad (p = p_c). \tag{2.10}$$

Proof. Most estimates here are proved in [39] except the second part of (2.7) when $p > p_c$. It can be proved for $p \in (1, p_{\max})$ by modifying the proof of [39, Prop. 2.7] for (2.8) as follows. (It is probably also well-known but we do not know a reference.)

Recall the ground state Q is obtained by the minimization problem (1.5). If a minimizer $Q(x)$ is rescaled so that

$$\frac{\int |\nabla Q|^2}{2a} = \frac{\int Q^2}{2b} = \frac{\int Q^{p+1}}{p+1} = \text{constant } k > 0,$$

i.e., (1.4) is satisfied, then $Q(x)$ satisfies (1.3). The minimization inequality $\frac{d^2}{d\varepsilon^2}\big|_{\varepsilon=0} J[Q + \varepsilon\eta] \geq 0$ for all real functions η, is equivalent to

$$k(\eta,\, L_+\eta) \geq \frac{1}{a}(\int \eta \Delta Q)^2 + \frac{1}{b}(\int Q\eta)^2 - (\int Q^p \eta)^2. \tag{2.11}$$

Thus $(\eta,\, L_+\eta) \geq 0$ if $\eta \perp Q^p$. Note that, if $\eta \perp Q$, by (1.3) the right side of (2.11) is positive if $a \leq 1$, i.e. $p \leq p_c$. In this way, we recover (2.8). □

2.2 Variational formulations of the eigenvalue problem for $\mathcal{L}$

In this subsection we summarize various variational formulations for eigenvalues of $\mathcal{L}$. The generalized nullspace is given by (2.5). Suppose $\lambda \neq 0$ is a (complex) eigenvalue of $\mathcal{L}$ with corresponding eigenfunction $\left[\begin{smallmatrix} u \\ w \end{smallmatrix}\right] \in L^2$,

$$\begin{bmatrix} 0 & L_- \\ -L_+ & 0 \end{bmatrix} \begin{bmatrix} u \\ w \end{bmatrix} = \lambda \begin{bmatrix} u \\ w \end{bmatrix}. \tag{2.12}$$

The functions u and w satisfy

$$L_+u = -\lambda w, \quad L_-w = \lambda u. \tag{2.13}$$

Therefore

$$L_-L_+u = \mu u, \quad \mu = -\lambda^2. \tag{2.14}$$

Since $(\mu u, Q) = (L_-L_+u, Q) = (L_+u, L_-Q) = 0$ and $\mu \neq 0$, we have $u \perp Q$.

Denote by Π the L^2-orthogonal projection onto $Q^\perp$. We can write $L_+u = \Pi L_+u + \alpha Q$. Eq. (2.14) implies $L_-\Pi L_+u = \mu u$ and hence, using $u \perp Q$ and (2.6), $\Pi L_+u = L_-^{-1}\mu u$. Thus

$$(u, Q) = 0, \quad L_+u = \mu L_-^{-1}u + \alpha Q. \tag{2.15}$$

Since (2.14) is also implied by Eq. (2.15), these two equations are equivalent.

If $Q(x)$ is a general solution of (1.3), $\mu = -\lambda^2$ may not be real. However, it must be real for the nonlinear ground state $Q = Q_{0,0,p}$. This fact is already known (see [29]). We will give a different proof.

Lemma. For $Q = Q_{0,0,p}$, every eigenvalue μ of (2.14) is real.

A new proof. Multiply (2.13) by $\bar{u}$ and $\bar{w}$ respectively and integrate. Then we get

$$(u, L_+u) = -\lambda(u, w), \quad (w, L_-w) = \lambda(w, u) = \lambda\overline{(u, w)}. \tag{2.16}$$

Taking the product, we get

$$(u, L_+u)(w, L_-w) = -\lambda^2|(u, w)|^2 = \mu|(u, w)|^2.$$

If $\mu \neq 0$, w is not a multiple of Q, and so by (2.6), $(w, L_-w) > 0$. Hence $(u, w) \neq 0$ by (2.16). Thus

$$\mu = \frac{(u, L_+u)(w, L_-w)}{|(u, w)|^2} \in \mathbb{R}.$$

□

This argument does not work when Q is an excited state, since (u, w) may be zero (see e.g. [37, Eq.(2.63)]). The fact $\mu \in \mathbb{R}$ implies that eigenvalues λ of $\mathcal{L}$ are either real or purely imaginary. Thus $\mathcal{L}$ has no complex eigenvalues with nonzero real and imaginary parts. This is not the case for excited states (see Section 4, also [37]).

The proof of reality of μ in [29] uses the following formulation. For the nonlinear ground state Q, L_- is nonnegative and the operator $L_-^{1/2}$ is defined on L^2 and invertible on $Q^\perp$. A nonzero $\mu \in \mathbb{C}$ is an eigenvalue of (2.14) if and only if it is also an eigenvalue of the following problem:

$$L_-^{1/2}L_+L_-^{1/2}g = \mu g, \tag{2.17}$$

with $g = L_-^{-1/2}u$. The operator $L_-^{1/2}L_+L_-^{1/2}$ already appeared in [36]. Since it can be realized as a self-adjoint operator, μ must be real.

Furthermore, the eigenvalues of $L_-^{1/2}L_+L_-^{1/2}$ can be counted using the minimax principle. Note that Q is an eigenfunction with eigenvalue 0. For easy comparison with other formulations, we formulate the principle on $Q^\perp$. Let

$$\mu_j := \inf_{g\perp Q, g_k, k=1,\dots,j-1} \frac{(g, L_-^{1/2}L_+L_-^{1/2}g)}{(g,g)}, \qquad (j=1,2,3,\dots) \tag{2.18}$$

with a suitably normalized minimizer denoted by g_j (if it exists – the definition terminates once a minimizer fails to exist). The corresponding definition for (2.15) is

$$\mu_j := \inf_{u\perp Q,\,(u,\,L_-^{-1}u_k)=0,\,k=1,\dots,j-1} \frac{(u, L_+u)}{(u, L_-^{-1}u)}, \qquad (j=1,2,3,\dots) \tag{2.19}$$

with a suitably normalized minimizer denoted by u_j (if it exists). In fact, the minimizer u_j satisfies

$$L_+u_j = \mu_j L_-^{-1}u_j + \alpha_j Q + \beta_1 L_-^{-1}u_1 + \cdots + \beta_{j-1}L_-^{-1}u_{j-1}, \tag{2.20}$$

for some Lagrange multipliers $\beta_1,\dots\beta_{j-1}$. Testing (2.20) with u_k with $k<j$, we get $(u_k, \beta_k L_-^{-1}u_k) = (u_k, L_+u_j) = (L_+u_k, u_j) = 0$ by (2.20) for u_k and the orthogonality conditions. Thus $\beta_k = 0$ and $L_+u_j = \mu_j L_-^{-1}u_j + \alpha_j Q$ and hence u_j satisfies (2.15).

Lemma 2.3 *The eigenvalues of* (2.18) *and* (2.19) *are the same, and*

$$\begin{aligned} \text{if } 1<p<p_c: &\quad \mu_1=\cdots=\mu_n=0, \quad \mu_{n+1}>0.\\ \text{if } p=p_c: &\quad \mu_1=\cdots=\mu_{n+1}=0, \quad \mu_{n+2}>0.\\ \text{if } p_c<p<p_{\max}: &\quad \mu_1<0, \quad \mu_2=\cdots=\mu_{n+1}=0, \quad \mu_{n+2}>0. \end{aligned}$$

The 0*-eigenspaces are span* $L_-^{-1/2}\{\nabla Q, \delta_{p_c}^p Q_1\}$ *for* (2.18) *and span*$\{\nabla Q, \delta_{p_c}^p Q_1\}$ *for* (2.19)*, where* $\delta_{p_c}^p$ *is defined in* (2.4)*.*

Proof. The eigenvalues of (2.18) and (2.19) are seen to be the same by taking $g = L_-^{-1/2}u$ up to a factor. By estimate (2.8), $\mu_1 \ge 0$ for $p\in(1,p_c]$. For $p\in(p_c,p_{\max})$, using (1.4), $\Pi Q_1 = Q_1 - \frac{(Q_1,Q)}{(Q,Q)}Q$, and elementary computations (such as (2.22) below), one finds

$$(\Pi Q_1, L_+\Pi Q_1) = \frac{n^2(p-1)}{4}(p_c-p)\frac{1}{p+1}\int Q^{p+1}$$

which is negative for $p>p_c$. Thus $\mu_1<0$. By estimate (2.7), $\mu_2\ge 0$ for $p\in(1,p_{\max})$.

It is clear that $u = \frac{\partial}{\partial x_j}Q$, $j=1,\dots,n$, provides n 0-eigenfunctions. For $p=p_c$, another 0-eigenfunction is $u=Q_1$ since $Q_1\perp Q$ (see again (2.22) below), $L_-^{-1}\nabla Q = -\frac{1}{2}xQ$, and $(Q_1, L_+Q_1)=0$. It remains to show that $\mu_{n+1}>0$ for $p\in(1,p_c)$ and $\mu_{n+2}>0$ for $p\in[p_c,p_{\max})$. If $\mu_{n+2}=0$ for $p\in(p_c,p_{\max})$, the argument after (2.20) shows the existence of a function $u_{n+2}\neq 0$ satisfying

$$L_+u_{n+2} = \alpha Q \quad \text{for some } \alpha\in\mathbb{R}, \quad u_{n+2}\perp Q,\, L_-^{-1}u_1,\, L_-^{-1}\nabla Q = -\tfrac{1}{2}xQ.$$

By Lemma 2.1, $u_{n+2} + \frac{\alpha}{2}Q_1 = c\cdot\nabla Q$ for some $c\in\mathbb{R}^d$. The orthogonality conditions imply $u_{n+2}=0$. The cases $p\in(1,p_c]$ are proved similarly. □

Remark 2.4 The formulation (2.19) for μ_1 has been used for the stability problem, see e.g. [34, p.73, (4.1.9)], which can be used to prove that $\mu_1 < 0$ if and only if $p \in (p_c, p_{\max})$ by a different argument. The later fact also follows from [39, 12] indirectly.

We summarize our previous discussion in the following theorem.

Summary 2.5 *Let $Q(x)$ be the unique positive radial ground state solution of* (1.3)*, and let $\mathcal{L}$, L_+ and L_- be as in* (1.8) *and* (1.10)*. The eigenvalue problems* (2.14)*,* (2.15)*, and* (2.17) *for $\mu \neq 0$ are equivalent, and the eigenvalues μ must be real. These eigenvalues can be counted by either* (2.18) *or* (2.19)*. $\mu_1 < 0$ if and only if $p \in (p_c, p_{\max})$. Furthermore, all eigenvalues of $\mathcal{L}$ are purely imaginary except for an additional real pair when $p \in (p_c, p_{\max})$.*

The last statement follows from the relation $\mu = -\lambda^2$ in (2.14).

2.3 Spectrum near 0 for p near p_c

We now consider eigenvalues of $\mathcal{L}$ near 0 when p is near p_c. It was suggested by M.I. Weinstein that as p approaches p_c from below, a pair of purely imaginary eigenvalues will collide at the origin, and split into a pair of real eigenvalues for $p > p_c$. In the following theorem and corollary we prove this picture rigorously and identify the leading terms of the eigenvalues and eigenfunctions.

Note that Comech-Pelinovsky [6] considers a different problem where the equation is fixed and the varying parameter is frequence ω rather than exponent p of the nonlinearity. That problem has only $U(1)$ symmetry and no translation, but its situation is similar to ours since we consider radial functions only in our proof. It seems one can adapt their approach to give an alternative proof. They use an abstract projection (Riesz projection) onto the discrete spectrum to reduce the problem to a 4x4 matrix problem (and exploit the complex structure), while we are more direct. We thank the referee for pointing out [6] to us.

Theorem 2.6 *There are small constants $\mu_* > 0$ and $\varepsilon_* > 0$ so that for every $p \in (p_c - \varepsilon_*, p_c + \varepsilon_*)$, there is a solution of*

$$L_+ L_- w = \mu w \tag{2.21}$$

of the form

$$w = w_0 + (p - p_c)^2 g, \quad w_0 = Q + a(p - p_c)|x|^2 Q, \quad g \perp Q,$$

$$\mu = 8a(p - p_c) + (p - p_c)^2 \eta, \quad a = a(p) = \frac{n(Q_1, Q^p)}{4(Q_1, x^2 Q)} < 0,$$

with $\|g\|_{L^2}$, $|\eta|$, $|a|$ and $1/|a|$ uniformly bounded in p. Moreover, for $p \neq p_c$, this is the unique solution of (2.21) *with $0 < |\mu| \leq \mu_*$.*

Proof. Set $\varepsilon := p - p_c$. Computations yield

$$(Q_1, Q) = \left(\frac{2}{p-1} - \frac{n}{2}\right)(Q, Q) = -\frac{\varepsilon n}{2(p-1)}(Q, Q), \tag{2.22}$$

$$(Q_1, Q^p) = -\frac{1}{p-1}(L_+Q, Q_1) = -\frac{1}{p-1}(Q, L_+Q_1) = \frac{2}{p-1}(Q, Q), \tag{2.23}$$

and

$$(Q_1, |x|^2Q) = \left(\frac{2}{p-1} - \frac{n+2}{2}\right)(Q, |x|^2Q) = -(1 + \frac{\varepsilon n}{2(p-1)})(Q, |x|^2Q). \tag{2.24}$$

Since by (2.21) with $\mu \neq 0$,

$$(Q_1, w) = \mu^{-1}(Q_1, L_+L_-w) = \mu^{-1}(L_-L_+Q_1, w) = 0,$$

we require the leading term $(Q_1, w_0) = 0$, which decides the value of a using (2.22) and (2.24). Thus we also need $(Q_1, g) = 0$. That $a < 0$ (at least for ε sufficiently small) follows from (2.23) and (2.24).

Using the computations

$$L_-|x|^2Q = [L_-, |x|^2]Q = -4x \cdot \nabla Q - 2nQ = -4Q_1 - \frac{2n}{p-1}\varepsilon Q \tag{2.25}$$

and

$$L_+Q = [L_- - (p-1)Q^{p-1}]Q = -(p-1)Q^p,$$

we find

$$L_+L_-w_0 = a\varepsilon L_+[-4Q_1 - \frac{2n}{p-1}\varepsilon Q] = a\varepsilon[8Q + 2n\varepsilon Q^p].$$

Thus $\mu = 8a\varepsilon + o(\varepsilon)$ and we need to solve

$$0 = [L_+L_- - 8a\varepsilon - \varepsilon^2\eta][w_0 + \varepsilon^2 g]$$

which yields our main equation for g and η:

$$L_+L_-g = 8a^2(|x|^2Q) - 2an(Q^p) + \eta w_0 + (8a\varepsilon + \varepsilon^2\eta)g. \tag{2.26}$$

Recall that on radial functions (we will only work on radial functions here)

$$\ker[(L_+L_-)^*] = \ker[L_-L_+] = \text{span}\{Q_1\}.$$

Let P denote the L^2-orthogonal projection onto Q_1 and $\bar{P} := \mathbf{1} - P$. It is necessary that

$$P[8a^2(|x|^2Q) - 2an(Q^p) + \eta w_0 + (8a\varepsilon + \varepsilon^2\eta)g] = 0$$

for (2.26) to be solvable. This solvability condition holds since $(Q_1, g) = (Q_1, w_0) = 0$, and, using the relations (2.24) and (2.23), $(Q_1, 8a^2(|x|^2Q) - 2an(Q^p)) = 0$.

Consider the restriction (on radial functions)

$$T = L_+L_- : \ [\ker L_-]^\perp = Q^\perp \longrightarrow Ran(\bar{P}) = Q_1^\perp.$$

Its inverse $T^{-1} = (L_-)^{-1}(L_+)^{-1}$ is bounded because $(L_+)^{-1} : Q_1^\perp \to Q^\perp$ and $(L_-)^{-1} : Q^\perp \to Q^\perp$ are bounded. So our strategy is to solve (2.26) as

$$g = T^{-1}\bar{P}[8a^2(|x|^2Q) - 2an(Q^p) + \eta w_0 + (8a\varepsilon + \varepsilon^2\eta)g] \tag{2.27}$$

by a contraction mapping argument, with η chosen so that $(Q_1, g) = 0$. Specifically, we define a sequence $g_0 = 0$, $\eta_0 = 0$, and

$$\begin{aligned} g_{k+1} &= \bar{P}T^{-1}\bar{P}[8a^2(|x|^2Q) - 2an(Q^p) + \eta_k w_0 + (8a\varepsilon + \varepsilon^2\eta_k)g_k], \\ \eta_{k+1} &= -\frac{1}{(Q_1, T^{-1}w_0)}\,(Q_1, T^{-1}\bar{P}[8a^2(|x|^2Q) - 2an(Q^p) + (8a\varepsilon + \varepsilon^2\eta_k)g_k]). \end{aligned}$$

We need to check $(Q_1, T^{-1}w_0)$ is of order one. Since $w_0 = Q + O(\varepsilon)$ and $L_+Q_1 = -2Q$, we have $(L_+)^{-1}w_0 = -\frac{1}{2}\Pi Q_1 + O(\varepsilon)$ where Π denotes the orthogonal projection onto $Q^\perp$. Thus, using (2.25) and (2.22),

$$\begin{aligned} (Q_1, T^{-1}w_0) &= -\frac{1}{2}(Q_1, (L_-)^{-1}\Pi Q_1) + O(\varepsilon) \\ &= \frac{1}{8}(Q_1, \Pi|x|^2Q) + O(\varepsilon) = \frac{1}{8}(Q_1, |x|^2Q) + O(\varepsilon), \end{aligned}$$

which is of order one because of (2.24). One may then check that $N_k := \|g_{k+1} - g_k\|_{L^2} + \varepsilon^{1/2}|\eta_{k+1} - \eta_k|$ satisfies $N_{k+1} \le C\varepsilon^{1/2}N_k$, and hence (g_k, η_k) is indeed a Cauchy sequence.

Finally, the uniqueness follows from the invariance of the total dimension of generalized eigenspaces near 0 under perturbations. □

Remark 2.7 To understand heuristically the leading terms in w and μ, consider the following analogy. Let $A_\varepsilon = \begin{bmatrix} 0 & 1 \\ 0 & \varepsilon \end{bmatrix}$, which corresponds to L_+L_-. One has $A_\varepsilon \left[\begin{smallmatrix} 1 \\ 0 \end{smallmatrix}\right] = \left[\begin{smallmatrix} 0 \\ 0 \end{smallmatrix}\right]$, $A_\varepsilon \left[\begin{smallmatrix} 0 \\ 1 \end{smallmatrix}\right] = \left[\begin{smallmatrix} 1 \\ \varepsilon \end{smallmatrix}\right]$ and $A_\varepsilon \left[\begin{smallmatrix} 1 \\ \varepsilon \end{smallmatrix}\right] = \varepsilon \left[\begin{smallmatrix} 1 \\ \varepsilon \end{smallmatrix}\right]$. The vectors $\left[\begin{smallmatrix} 1 \\ 0 \end{smallmatrix}\right]$, $\left[\begin{smallmatrix} 0 \\ 1 \end{smallmatrix}\right]$ and $\left[\begin{smallmatrix} 1 \\ \varepsilon \end{smallmatrix}\right]$ correspond to Q, $|x|^2Q$ and w, respectively.

The theorem yields an eigenvalue μ with the same sign as $p_c - p$. Since the eigenvalues of $\mathcal{L}$ are given by $\lambda = \pm\sqrt{-\mu}$, we have the following corollary.

Corollary 2.8 *With notations as in Theorem 2.6, $\mathcal{L}$ has a pair of eigenvalues $\lambda = \pm\sqrt{-\mu} = \pm\sqrt{8|a|(p - p_c) - (p - p_c)^2\eta}$ with corresponding eigenvectors $\left[\begin{smallmatrix} u \\ w \end{smallmatrix}\right]$ solving* (2.12) *and*

$$u = \lambda^{-1}L_-w = \mp\sqrt{2|a|(p - p_c)}\,Q_1 + O((p - p_c)^{3/2}).$$

When $p \in (p_c - \varepsilon_*,\ p_c)$ (stable case), λ and u are purely imaginary.
When $p \in (p_c,\ p_c + \varepsilon_*)$ (unstable case), λ and u are real.

In deriving the leading term of u we have used (2.25). We solved for w before u simply because w is larger than u.

3 One dimensional theory

In this section we focus on the one dimensional theory. For $n = 1$, the ground state $Q(x)$ has an explicit formula for all $p \in (1, \infty)$,

$$Q(x) = c_p \cosh^{-\beta}(x/\beta), \quad c_p := (\frac{p+1}{2})^{\frac{1}{p-1}}, \quad \beta := \frac{2}{p-1}. \tag{3.1}$$

The function $Q(x)$ satisfies (1.3) and is the unique $H^1(\mathbb{R})$-solution of (1.3) up to translation and phase [4, p.259, Theorem 8.1.6].

3.1 Eigenfunctions of L_+ and L_-

We first consider eigenvalues and eigenfunctions of L_+ and L_-. For $n = 1$,

$$L_+ = -\partial_{xx} + 1 - pQ^{p-1}, \qquad L_- = -\partial_{xx} + 1 - Q^{p-1}. \tag{3.2}$$

By (3.1), these operators are both of the form

$$-\partial_{xx} + 1 - C \operatorname{sech}^2(x/\beta).$$

Such operators have essential spectrum $[1, \infty)$, and finitely many eigenvalues below 1. A lot of information about such operators is available in the classical book [35], p. 103:

- all eigenvalues are simple, and can be computed explicitly, as zeros and poles of an explicit meromorphic function;
- all eigenfunctions can be expressed in terms of the hypergeometric function.

We begin by presenting another way to derive the eigenvalues, as well as different formulas for the eigenfunctions. We will not prove right here that this set contains all of the eigenvalues/eigenfunctions. This fact is a consequence of the more general Theorem 3.4, proved later (and see also [35]).

Define

$$\begin{aligned} &\lambda_m := 1 - k_m^2, \qquad k_m := \frac{p+1}{2} - \frac{m(p-1)}{2}, \\ &p_m := \frac{m+1}{m-1} \quad \text{for } m > 1, \quad p_1 = \infty. \end{aligned} \tag{3.3}$$

The following theorem agrees with the numerical observation Figure 1.

Theorem 3.1 *For $n = 1$ and $1 < p < \infty$, let $Q(x)$ be defined by (3.1), L_+ and L_- be defined by (3.2), and λ_m, k_m, p_m be defined by (3.3). Suppose for $M \in \mathbb{Z}^+$,*

$$p_{M+1} \le p < p_M. \tag{3.4}$$

Then the operator L_+ has eigenvalues λ_m, $0 \le m \le M$, with eigenfunctions of the form

$$\varphi_{2\ell} = \sum_{j=0}^{\ell} c_{2j}^{2\ell} Q^{k_{2j}}, \quad \varphi_{2\ell-1} = \sum_{j=1}^{\ell} c_{2j-1}^{2\ell-1} (Q^{k_{2j-1}})_x,$$

and the operator L_- has eigenvalues λ_m, $1 \le m \le M$, with eigenfunctions of the form

$$\psi_{2\ell-1} = \sum_{j=1}^{\ell} d_{2j-1}^{2\ell-1} Q^{k_{2j-1}}, \qquad \psi_{2\ell} = \sum_{j=1}^{\ell} d_{2j}^{2\ell} (Q^{k_{2j}})_x.$$

In particular, all eigenvalues of L_- are eigenvalues of L_+, and L_+ always has one more eigenvalue ($\lambda_0 < 0$) than L_-.

Proof. It can be proved by induction, using

$$Q^{p-1} = \frac{p+1}{2}\,\cosh^{-2}(x/\beta), \quad Q_x = -Q\tanh(x/\beta), \quad Q_x^2 = Q^2(1 - \frac{2}{p+1}Q^{p-1}),$$

and

$$Q^{-k} L_+ Q^k = \frac{(k+p)\,(2k-p-1)}{p+1}\,Q^{p-1} + (1-k^2), \tag{3.5}$$

$$[(Q^k)_x]^{-1} L_+ (Q^k)_x = \frac{(k-1)(2k+3p-1)}{p+1}\,Q^{p-1} + (1-k^2),$$

$$Q^{-k} L_- Q^k = \frac{(k-1)(2k+p+1)}{p+1}\,Q^{p-1} + (1-k^2), \tag{3.6}$$

$$[(Q^k)_x]^{-1} L_- (Q^k)_x = \frac{(k+p)(2k+p-3)}{p+1}\,Q^{p-1} + (1-k^2).$$

The coefficients of Q^{p-1} vanish when $k = \frac{p+1}{2}, 1, 1, \frac{3-p}{2}$, respectively. It is why the highest power of Q is $Q^{\frac{p+1}{2}}$ in $\varphi_{2\ell}$, Q_x in $\phi_{2\ell-1}$, Q in $\psi_{2\ell-1}$, and $(Q^{\frac{3-p}{2}})_x$ in $\psi_{2\ell}$. □

3.2 Connection between L_+ and L_- and their factorizations

In light of Theorem 3.1, it is natural to ask *why* all eigenvalues of L_- are also eigenvalues of L_+. Is there a simple connection between their eigenfunctions? In this section we prove this is indeed so.

We first look for an operator U of the form

$$U = \partial_x + R(x), \qquad (\text{ so } U^* = -\partial_x + R(x)),$$

such that

$$L_- U = U L_+, \qquad (\text{ so } U^* L_- = L_+ U^*). \tag{3.7}$$

It turns out that there is a unique choice of $R(x)$:

$$R(x) = -\frac{p+1}{2}\frac{Q_x}{Q} = \frac{p+1}{2}\tanh(\frac{(p-1)x}{2}).$$

In fact, with this choice of $R(x)$,

$$U = \varphi_0 \partial_x \varphi_0^{-1}, \qquad (\text{ so } U^* = -\varphi_0^{-1}\partial_x\varphi_0), \tag{3.8}$$

where $\varphi_0 = Q^{\frac{p+1}{2}}$ is the ground state of L_+, and is considered here as a multiplication operator: $Uf = \varphi_0\partial_x(\varphi_0^{-1}f)$.

Suppose now ψ is an eigenfunction of L_- with eigenvalue λ: $L_-\psi = \lambda\psi$. By (3.7),

$$0 = U^*(L_- - \lambda)\psi = (L_+ - \lambda)U^*\psi.$$

Thus $U^*\psi$ is an eigenfunction of L_+ with same eigenvalue λ (provided $U^*\psi \in L^2$). Therefore, the map

$$\psi \mapsto U^*\psi$$

sends an eigenfunction of L_- to an eigenfunction of L_+ with same eigenvalue. This map is not onto because U^* is not invertible. Specifically, the ground state φ_0 is not in the range. In fact, $U\varphi_0 = \varphi_0\partial_x\varphi_0^{-1}\varphi_0 = 0$. If $\varphi_0 = U^*\psi$, then $(\varphi_0, \varphi_0) = (\varphi_0, U^*\psi) = (U\varphi_0, \psi) = 0$, a contradiction. We summarize our finding as the following proposition.

Proposition 3.2 *Under the same assumptions and notation as Theorem 3.1, the eigenfunctions φ_m and ψ_m of L_+ and L_- satisfy*

$$\varphi_m = U^*\psi_m, \qquad (m = 1, \ldots, M),$$

up to constant factors. Note that U^* sends even functions to odd functions and vice versa.

Proof. We only need to verify that $U^*\psi_m \in L^2$. This is the case since $U^* = -\partial_x + \frac{p+1}{2}\tanh(x/\beta)$, $\psi_m(x)$ are sums of powers of Q and Q_x, and that $\tanh(x/\beta)$, Q_x/Q, and Q_{xx}/Q_x are bounded. □

Analogous to the definition of U, we define

$$S := Q\partial_x Q^{-1} = \partial_x - \frac{Q_x}{Q}, \qquad (\text{ so } S^* = -Q^{-1}\partial_x Q). \tag{3.9}$$

Clearly $SQ = 0$. Recall that λ_0 is the first eigenvalue of L_+ with eigenfunction φ_0. Hence $L_+ - \lambda_0$ is a nonnegative operator. In fact we have the following factorizations.

Lemma 3.3 *Let U and S be defined by* (3.8) *and* (3.9)*, respectively. One has*

$$L_+ - \lambda_0 = U^*U, \qquad L_- - \lambda_0 = UU^*. \tag{3.10}$$

$$L_- = S^*S, \qquad SS^* = -\partial_x^2 + 1 + \frac{p-3}{p+1}Q^{p-1}. \tag{3.11}$$

Moreover, $SS^* = L_- + \frac{2(p-1)}{p+1}Q^{p-1} > 0$.

The formula $L_- = S^*S$ was known, see e.g. [34, p.73, (4.1.8)]. It is an example of the Darboux transformations, see e.g. [22]. Factorization of Schrödinger operators into first-order operators has been known since the times of Darboux (1840s).

3.3 Hierarchy of Operators

In this subsection we generalize Theorem 3.1 and Lemma 3.3 to a family of operators containing L_+ and L_-. As a reminder, we have

$$\begin{aligned} &Q''/Q = 1 - Q^{p-1}, \quad (Q'/Q)^2 = 1 - \frac{2}{p+1}Q^{p-1}, \\ &(Q'/Q)' = Q''/Q - (Q'/Q)^2 = -\frac{p-1}{p+1}Q^{p-1}. \end{aligned} \tag{3.12}$$

Let $S(a) := Q^a \partial_x Q^{-a}$. We have

$$\begin{aligned} &S(a) = \partial_x - aQ'/Q, \ S(a)^* = -\partial_x - aQ'/Q, \\ &S(a)^*S(a) = -\partial_x^2 + a^2 - a\left\{a + \frac{p-1}{2}\right\}\frac{2}{p+1}Q^{p-1}. \end{aligned} \tag{3.13}$$

Define the following hierarchy of operators:

$$\begin{aligned} &S_j := S(k_j), \quad \text{where recall} \quad k_j = 1 - (j-1)\frac{p-1}{2}, \\ &L_j := S_{j-1}S_{j-1}^* + \lambda_{j-1} = S_j^*S_j + \lambda_j, \quad \text{where recall} \quad \lambda_j = 1 - k_j^2. \end{aligned} \tag{3.14}$$

Then we have

$$\begin{aligned} &S_0 = U, \ S_1 = S, \dots \\ &L_0 = L_+, \ L_1 = L_-, \ L_2 = SS^*, \dots \\ &S_jL_j = L_{j+1}S_j, \quad L_jS_j^* = S_j^*L_{j+1}. \end{aligned} \tag{3.15}$$

More explicitly,

$$L_j = -\partial_x^2 + 1 - k_{j-1}k_j\frac{2}{p+1}Q^{p-1}. \tag{3.16}$$

Note that j here can be any real number.

Recall the definition $p_j := 1 + 2/(j-1)$ for $j > 1$, and set $p_j = \infty$ for $j \le 1$. Then p_j is a monotone decreasing function of j, $k_j > 0$ for $p < p_j$, $k_j = 0$ for $p = p_j$ and $k_j < 0$ for $p > p_j$. Let

$$\lambda_j' := \begin{cases} \lambda_j & (1 < p \le p_j), \\ 1 & (p_j < p < p_{j-1}), \\ \lambda_{j-1} & (p_{j-1} \le p). \end{cases} \tag{3.17}$$

By the second identity of (3.14), and (3.16) together with the fact $k_{j-1}k_j < 0$ for $p_j < p < p_{j-1}$, we have the lower bound

$$L_j \geq \lambda'_j. \tag{3.18}$$

In fact, this estimate is sharp: for $p \in (1, p_j) \cup (p_{j-1}, \infty)$, the ground state is obvious from the second identity of (3.14):

$$\begin{cases} L_j Q_j = \lambda_j Q_j, & (1 < p < p_j), \\ L_j Q_{j-1}^* = \lambda_{j-1} Q_{j-1}^*, & (p_{j-1} < p), \end{cases} \tag{3.19}$$

where we denote

$$Q_j := Q^{k_j}, \quad Q_j^* := Q^{-k_j}. \tag{3.20}$$

For $p \in [p_j, p_{j-1}]$, there is no ground state. Thus we have completely determined the ground state of L_j for all $p > 1$. The complete spectrum, together with explicit eigenfunctions, are derived using the third identity of (3.15) as follows.

Theorem 3.4 *For any $j \in \mathbb{R}$ and $p > 1$, the point spectrum of L_j consists of simple eigenvalues*

$$\begin{aligned} spec_p(L_j) = &\{\lambda_k \mid p < p_k,\ k \in \{j, j+1, j+2, \dots\}\} \\ &\cup \{\lambda_k \mid p > p_k,\ k \in \{j-1, j-2, j-3, \dots\}\}, \end{aligned} \tag{3.21}$$

and the eigenfunction for the eigenvalue λ_k is given uniquely up to constant multiple by

$$\begin{cases} S_j^* \cdots S_{k-1}^* Q_k & (k \in \{j, j+1, \dots\}), \\ S_{j-1} \cdots S_{k+1} Q_k^* & (k \in \{j-1, j-2, \dots\}), \end{cases} \tag{3.22}$$

each of which is a linear combination of

$$\begin{cases} Q_j, Q_{j+2}, \dots Q_k & (k \in \{j, j+2, \dots\}), \\ Q_{j+1}R, Q_{j+3}R, \dots Q_k R & (k \in \{j+1, j+3, \dots\}), \\ Q_{j-1}^*, Q_{j-3}^*, \dots Q_k^* & (k \in \{j-1, j-3, \dots\}), \\ Q_{j-2}^* R, Q_{j-4}^* R, \dots Q_k^* R & (k \in \{j-2, j-4, \dots\}) \end{cases} \tag{3.23}$$

where $R := Q'/Q$.

Proof. The ground states have been determined. The third identity of (3.15) implies that (3.22) belong to the eigenspace of L_j with eigenvalue λ_k. Moreover, each function is nonzero because S_k^* is injective for $p < p_k$ and so is S_k for $p_k < p$. Since S_j annihilates only the ground state Q_j for $p < p_j$ and S_{j-1}^* annihilates only the ground state Q_{j-1}^* for $p > p_j$, all the excited states of L_j for $p < p_j$ are mapped injectively by S_j to bound states of L_{j+1}, and for $p > p_j$ by S_{j-1}^* to those of L_{j-1}. Hence we have (3.21) and all the eigenvalues are simple because the ground states are so. (3.23) follows from the fact that S_j and S_j^* act on Q^a like $C(a,j)R$, while $S_j S_{j-1}$ and $S_{j-1}^* S_j^*$ act on Q^a like $C_1(a,j) + C_2(a,j)Q^{p-1}$. □

3.4 Mirror conjugate identity

The following remarkable identity has application to estimating eigenvalues of $\mathcal{L}$ (see Section 3.6):

$$S_j(L_{j-1} - \lambda_j)S_j^* = S_j^*(L_{j+2} - \lambda_j)S_j. \tag{3.24}$$

To prove this, start with the formula

$$\begin{aligned}(\partial_x + R)(\partial_x^2 + V)(\partial_x - R) \\ = \partial_x^4 + (-3R' - R^2 + V)\partial_x^2 + (-3R' - R^2 + V)'\partial_x \\ - R''' - (VR)' - RR'' - R^2V,\end{aligned} \tag{3.25}$$

which implies that $(\partial_x + R)(\partial_x^2 + V_+)(\partial_x - R) = (\partial_x - R)(\partial_x^2 + V_-)(\partial_x + R)$ is equivalent to

$$V_\pm = -R''/R \pm 3R' - R^2 + C/R. \tag{3.26}$$

Now set $R := aQ'/Q$. Plugging the following identities

$$\begin{aligned}&R^2 = a^2(1 - \frac{2}{p+1}Q^{p-1}),\ R' = -a\frac{p-1}{p+1}Q^{p-1}, \\ &R''/R = -\frac{(p-1)^2}{p+1}Q^{p-1}.\end{aligned} \tag{3.27}$$

into (3.26), we get, for $C = 0$,

$$V_\pm = -a^2 + \frac{2}{p+1}(a \pm (p-1))(a \pm (p-1)/2)Q^{p-1}. \tag{3.28}$$

Hence for $a = k_j$ we have

$$V_\pm = -k_j^2 + \frac{2}{p+1}k_{j\pm2}k_{j\pm1}, \tag{3.29}$$

which gives the desired identity (3.24). The above proof also shows that L_{j-1} and L_{j+2} are the unique choice for the identity to hold with S_j (modulo a constant multiple of Q/Q_x, which is singular).

3.5 Variational formulations for eigenvalues of $\mathcal{L}$

We considered two variational formulations for nonzero eigenvalues of $\mathcal{L}$ in general dimensions in Section 2.2. Here we present a new variational formulation for 1-D. Define the selfadjoint operator

$$H := SL_+S^*. \tag{3.30}$$

This is a fourth-order differential operator, with essential spectrum $[1, \infty)$. By a direct check, we have

$$HQ = SL_+S^*Q = SL_+(-2Q_x) = 0.$$

Thus Q is an eigenfunction with eigenvalue 0. Since $(Q, S^*f) = (SQ, f) = 0$ for any f, we have

$$\text{Range } S^* \perp Q. \tag{3.31}$$

In particular, since $L_+|_{Q^\perp}$ is nonnegative for $p \le 5$ by Lemma 2.2, so is H.

Lemma 3.5 *The null space of H is*

$$N(H) = \mathit{span}\left\{Q, \delta^p_{p_c} xQ\right\},$$

where, recall, $\delta^p_{p_c}$ is 0 if $p \neq p_c$, and 1 if $p = p_c$.

Remark. Note that dim $N(H) = 1 + \delta^p_{p_c}$ which is different from dim $N(L_-^{1/2} L_+ L_-^{1/2}) = 2 + \delta^p_{p_c}$. We will show below that H and $L_-^{1/2} L_+ L_-^{1/2}$ have the same *nonzero* eigenvalues.

Proof. If $Hf = 0$, then $L_+ S^* f = -2cQ$ and $S^* f = cQ_1 + dQ_x$ for some $c, d \in \mathbb{R}$ by Lemma 2.1. We have $Q_1 \perp Q$ iff $p = p_c = 5$. Thus, if $p \neq 5$, $c = 0$ by (3.31), and $S^*(f + \frac{d}{2}Q) = 0$. We conclude $f = -\frac{d}{2}Q$.

When $p = 5$, we have $S^* xQ = -Q^{-1}\partial_x(QxQ) = -2Q_1$. Thus $S^*(f + \frac{c}{2}Q_1 + \frac{d}{2}Q) = 0$ and $f = -\frac{c}{2}Q_1 - \frac{d}{2}Q$. □

Define eigenvalues of H as follows:

$$\tilde{\mu}_j := \inf_{f \perp f_k, k<j} \frac{(f, Hf)}{(f, f)}, \qquad (j = 1, 2, 3, \ldots) \tag{3.32}$$

with a suitably normalized minimizer denoted by f_j, if it exists. By standard variational arguments, if $\tilde{\mu}_j < 1$, then a minimizer f_j exists. By convention, if μ_k is the first of the μ_j's to hit 1 (and so f_k may not be defined), we set $\mu_j := 1$ for all $j > k$.

We can expand Summary 2.5 to the following.

Theorem 3.6 (Equivalence) *Let $n = 1$. Let μ_j be defined as in Summary 2.5 and $\tilde{\mu}_j$ be defined by* (3.32)*. Then $\mu_j = \tilde{\mu}_j$. When $\mu_j \neq 0$ and $\mu_j < 1$, the eigenfunctions of* (2.19) *and* (3.32) *can be chosen to satisfy*

$$u_j = S^* f_j, \quad f_j = \frac{1}{\mu_j} SL_+ u_j.$$

Proof. First we establish the equivalence of nonzero eigenvalues. Suppose $f = f_j$ is an eigenfunction of (3.32) with eigenvalue $\tilde{\mu} \neq 0$, then $SL_+S^*f = \tilde{\mu}f$. Let $u := S^*f \neq 0$ and apply S^* on both sides. By $L_- = S^*S$ we get $L_-L_+u = \tilde{\mu}u$. Thus u is an eigenfunction satisfying (2.14) with $\mu = \tilde{\mu}$. On the other hand, suppose u satisfies $L_-L_+u = \mu u$ with $\mu \neq 0$. Applying SL_+ on both sides and using $L_- = S^*S$, we get $SL_+S^*SL_+u = \mu SL_+u$, i.e., $Hf = \mu f$ for $f = \mu^{-1}SL_+u$.

Now use Lemmas 2.3 and 3.5. If $p \in (1, 5)$, then $\mu_1 = \tilde{\mu}_1 = 0$, corresponding to Q_x and Q, and $\mu_2 = \tilde{\mu}_2 > 0$. If $p = 5$, then $\mu_1 = \mu_2 = \tilde{\mu}_1 = \tilde{\mu}_2 = 0$, corresponding to Q_x, Q_1, and

Q, xQ, and $\mu_3 = \tilde{\mu}_3 = 1$. If $p \in (5, \infty)$, then $\mu_1 = \tilde{\mu}_1 < 0$, $\mu_2 = \tilde{\mu}_2 = 0$, corresponding to Q_x and Q, and $\mu_3 = \mu_3 = 1$. We have shown $\tilde{\mu}_j = \mu_j$. □

In the following we will make no distinction between μ_j and $\tilde{\mu}_j$. By the minimax principle, (3.32) has the following equivalent formulations:

$$\mu_j = \inf_{\dim M = j} \sup_{f \in M} \frac{(f, Hf)}{(f, f)} = \sup_{\dim M = j-1} \inf_{f \perp M} \frac{(f, Hf)}{(f, f)}. \tag{3.33}$$

Here M runs over all linear subspaces of $L^2(\mathbb{R})$ with the specified dimension.

3.6 Estimates of eigenvalues of $\mathcal{L}$

In this subsection we prove lower and upper bounds for eigenvalues of $\mathcal{L}$, confirming some aspects of the numerical computations shown in Figure 1. Recall that, by Lemma 2.3, the first positive μ_j is μ_2 for $p \in (1, p_c)$ and μ_3 for $p \in [p_c, p_{\max})$. The first theorem concerns upper bounds for μ_1 and μ_2.

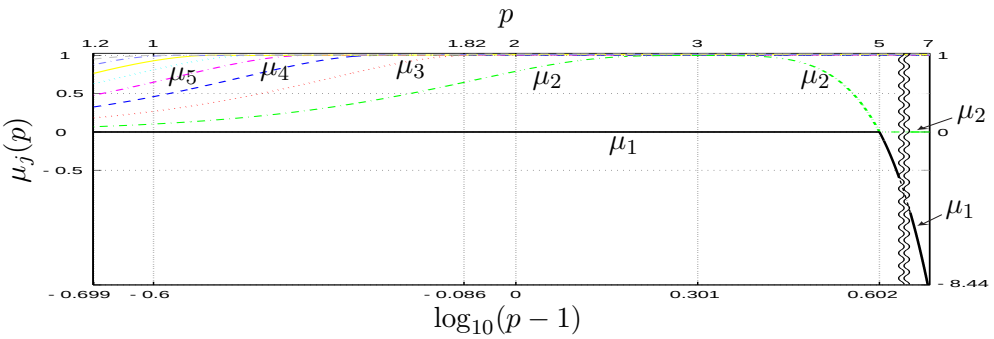

Figure 6: p vs. μ_j.

Theorem 3.7 *Suppose $n = 1$ and $1 < p < \infty$.*

(a) If $p \neq 3$, then $\mu_2 \leq C_p$ for some explicitly computable $C_p < 1$. In particular f_2 exists.

(b) $\mu_1 < 0$ if and only if $p > 5$. For any $C > 0$, we have $\mu_1(p) \leq -Cp^3$ for p sufficiently large.

Proof. For part (a), we already know $\mu_2 = 0$ for $p \geq 5$. Assume $p \in (1, 5)$. Consider test functions of the form $f = SQ^k$ with $k > 0$. f is odd and hence $f \perp Q$, the 0-eigenfunction of H. Since $H = SL_+S^*$ and $S^*S = L_-$, we have

$$\mu_2 \leq \frac{(f, Hf)}{(f, f)} = \frac{(L_-Q^k, L_+L_-Q^k)}{(Q^k, L_-Q^k)}.$$

By formulas (3.5) and (3.6),

$$L_-Q^k = aQ^{k+p-1} + bQ^k, \quad a = \frac{1}{p+1}(k-1)(2k+p+1), \quad b = 1 - k^2.$$

$$L_+ Q^{k+p-1} = \sigma Q^{k+2p-2} + d Q^{k+p-1},$$

$$\sigma = \frac{1}{p+1}(k+2p-1)(2k+p-3), \quad d = 1-(k+p-1)^2.$$

$$L_+ Q^k = c Q^{k+p-1} + b Q^k, \quad c = \frac{1}{p+1}(k+p)(2k-p-1).$$

Thus

$$\frac{(f,Hf)}{(f,f)} = \frac{a^2\sigma J_3 + a(ad+bc+b\sigma)J_2 + b(ad+ab+bc)J_1 + b^3 J_0}{aJ_1 + bJ_0} \tag{3.34}$$

where

$$J_m = \int_{\mathbb{R}} Q^{2k+m(p-1)}(x)\,dx, \quad (m=0,1,2,3),$$

which are always positive. If $k \to 0^+$, then J_m converges to $\int_{\mathbb{R}} Q^{m(p-1)}\,dx$ for $m>0$, and $J_0 = O(k^{-1})$. The above quotient can be written as

$$(3.34) = b^2 + \frac{J}{aJ_1 + bJ_0}$$

where

$$J = a^2\sigma J_3 + a(ad+bc+b\sigma)J_2 + b(ad+bc)J_1.$$

Note that $J_m|_{k=0} = (\frac{p+1}{2})^m \frac{2}{p-1} \int_{\mathbb{R}} \operatorname{sech}^{2m}(y)\,dy$ with $\int_{\mathbb{R}} \operatorname{sech}^{2m}(y)\,dy = 2, \frac{4}{3}, \frac{16}{15}$ for $m = 1,2,3$, respectively. Also, as $k \to 0^+$, $a \to -1$, $b \to 1$, $c \to -p$, $\sigma \to \frac{(2p-1)(p-3)}{p+1}$, and $d \to 1-(p-1)^2$. Direct calculation shows

$$\lim_{k\to 0^+} J = -\frac{2}{15(p-1)}\,(p+1)^2(p-3)^2.$$

Also note $b^2 < 1$ for $k>0$. Thus, if $1<p<\infty$ and $p \neq 3$, then $J<0$ and the quotient (3.34) is less than 1 for k sufficiently small. (If $p=3$, the sign of J is unclear and (3.34) may not be less than 1.) This proves $\mu_2 < 1$ and provides an upper bound less than 1 for μ_2. It also implies the existence of f_2. This establishes statement (a).

For statement (b), the fact that $\mu_1 < 0$ if and only if $p>5$ is part of Lemma 2.3. We now consider the behavior of μ_1 for p large. Fix $k>1$ to be chosen later. As $p \to \infty$,

$$J_m = (\frac{p+1}{2})^{\frac{2k}{p-1}+m} \cdot \frac{2}{p-1} \cdot \int_{\mathbb{R}} (\operatorname{sech} x)^{\frac{4k}{p-1}+2m}\,dx \sim C_m p^{m-1},$$

with $C_m = 2^{1-m}\int_{\mathbb{R}} (\operatorname{sech} x)^{2m} dx = 2, \frac{2}{3}, \frac{4}{15}$ for $m=1,2,3$, respectively, and

$$a \sim k-1, \quad b = 1-k^2, \quad c \sim -p, \quad \sigma \sim 2p, \quad d \sim -p^2.$$

Thus, by (3.34),

$$\frac{(f,Hf)}{(f,f)} \sim \frac{a\sigma J_3 + adJ_2}{J_1} \sim \frac{1-k}{15}\,p^3 \quad \text{as } p \to \infty.$$

By choosing $k > 1$ sufficiently large, we have shown that for any C, $\mu_1 \le -Cp^3$ for p sufficiently large. $\square$

The next theorem bounds eigenvalues of $\mathcal{L}$ by eigenvalues of L_+ and L_-. Recall p_j and $\lambda_j(p)$ are defined in (3.4) and (3.3).

Theorem 3.8 (Interlacing of eigenvalues) *Fix $k \ge 1$ and $p \in [p_{k+2},\ p_{k+1})$ where, recall, $p_j = \frac{j+1}{j-1}$. Let $\lambda_j(p) = 1 - \frac{1}{4}[(p+1) - j(p-1)]^2$ be as in (3.3) and so $\lambda_{k+1} < 1 \le \lambda_{k+2}$. For the eigenvalues μ_j defined by (3.32), we have*

$$\lambda_{j+1}^2(p) < \mu_{j+1}(p) < \lambda_{j+2}^2(p), \quad (1 \le j < k); \qquad \lambda_{k+1}^2(p) < \mu_{k+1}(p) \le 1. \tag{3.35}$$

In particular, there are K simple eigenvalues $\mu_2, \dots, \mu_{K+1}$ in $(0,1)$ where $K = k$ if $\mu_{k+1} < 1$ and $K = k-1$ if $\mu_{k+1} = 1$. Moreover, K is always 1 when $k = 1$. Finally,

$$\mu_2 \ge \begin{cases} \lambda_2\lambda_3 & (1 < p \le 2), \\ \lambda_2 & (2 < p < 5), \end{cases} \qquad \mu_3 \ge \begin{cases} \lambda_3\lambda_4 & (1 < p \le 5/3), \\ \lambda_3 & (5/3 < p \le 2), \\ 1 & (2 < p < \infty), \end{cases}$$

$$\mu_1 \ge -\frac{1}{16}(p-1)^3(p-5) \quad (5 \le p < \infty).$$

Remark 3.9 In view of the above lower bounds for μ_2 and μ_3, we conjecture that

$$\mu_{j+1} \ge \lambda_{j+1}\lambda_{j+2} \quad (1 < p < p_{j+2}); \qquad \mu_{j+1} \ge \lambda_{j+1} \quad (p_{j+2} \le p < p_{j+1}). \tag{3.36}$$

This is further confirmed numerically for $j = 3, 4, 5$ (see Figure 7). Note that $\lim_{p \to p_{j+1}-} \frac{\lambda_{j+1}}{\mu_{j+1}} = 1$ because both λ_{j+1} and μ_{j+1} converge to 1. It also seems that $\frac{\lambda_{j+1}\lambda_{j+2}}{\mu_{j+1}}$ has a limit as $p \to 1+$, but it is not clear although we have (3.35) and $\lambda_j = (j-1)(p-1) + O((p-1)^2)$ as $p \to 1+$.

Proof. We first prove the upper bound: For $j < k$, use the test functions

$$S\psi_2,\ S\psi_3,\ \dots,\ S\psi_{j+2}$$

(we cannot use $S\psi_1$ since it is zero). Recall $L_-\psi_m = \lambda_m\psi_m$. Let $a = (a_2, \dots, a_{j+2})$ vary over $\mathbb{C}^{j+1} - \{0\}$. By equivalent definition (3.33), $H = SL_+S^*$, $L_- = S^*S$, and the orthogonality between the ψ_m's, we have

$$\begin{aligned} \mu_{j+1} &\le \sup_a \frac{(\sum_m a_m S\psi_m, H\sum_\ell a_\ell S\psi_\ell)}{(\sum_m a_m S\psi_m, \sum_\ell a_\ell S\psi_\ell)} = \sup_a \frac{(\sum_m a_m\psi_m, L_-L_+L_-\sum_\ell a_\ell\psi_\ell)}{(\sum_m a_m\psi_m, L_-\sum_\ell a_\ell\psi_\ell)} \\ &\le \sup_a \frac{(\sum_m a_m\psi_m, L_-L_-L_-\sum_\ell a_\ell\psi_\ell)}{(\sum_m a_m\psi_m, L_-\sum_\ell a_\ell\psi_\ell)} = \sup_a \frac{\sum_m |a_m|^2\lambda_m^3}{\sum_m |a_m|^2\lambda_m} \\ &\le \max_{m=2,\dots,j+2} \lambda_m^2 = \lambda_{j+2}^2. \end{aligned}$$

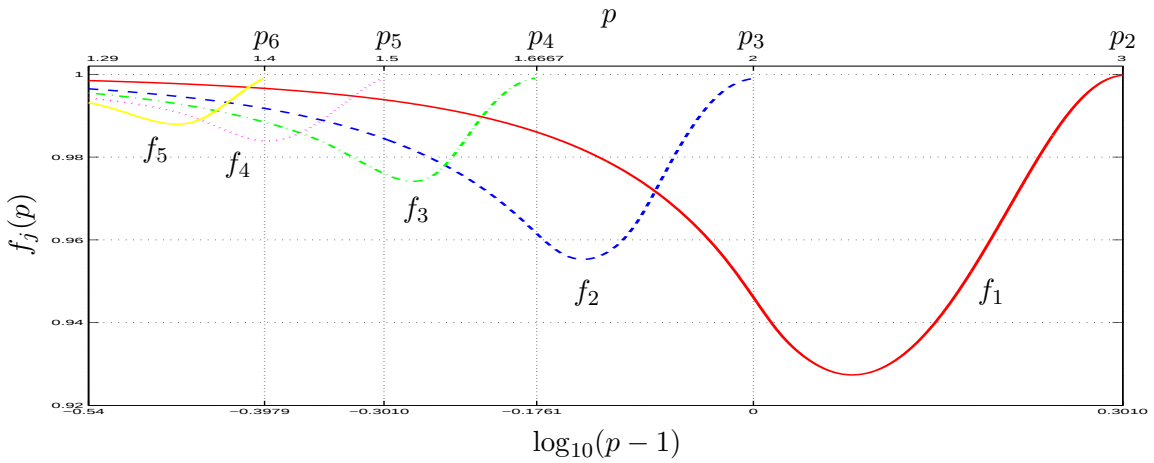

Figure 7: p vs. f_j for $j = 1, \ldots, 5$, where $f_j(p) = \frac{\lambda_{j+1}\lambda_{j+2}}{\mu_{j+1}}$ for $1 < p < p_{j+2}$ and $f_j(p) = \frac{\lambda_{j+1}}{\mu_{j+1}}$ for $p_{j+2} \le p < p_{j+1}$.

Since $\mu_{j+1} \le \lambda_{j+2}^2 < 1$, it is attained at some function, for which the second inequality above cannot be replaced by an equality sign. Thus $\mu_{j+1} < \lambda_{j+2}^2$.

For the lower bound of eigenvalues, we use only the special case $j = 1$ of (3.24):

$$H = SL_+S^* = SL_0S^* = S^*L_3S. \tag{3.37}$$

In particular, we have for $1 < p < 3$,

$$H \ge S^*L_2S = S^*SS^*S = L_1^2 = L_-^2, \tag{3.38}$$

which implies that

$$\lambda_{j+1}^2 \le \mu_{j+1} \quad (1 < p < 3) \tag{3.39}$$

(and again, equality is impossible).

For the second eigenvalue μ_2, we can get a more precise estimate by using (3.18) for $L_3 \ge \lambda_3'$ together with

$$L_1|_{Q^\perp} \ge \lambda_2', \tag{3.40}$$

which follows from $spec(L_1)$. Combining these estimates, we have for any $f \perp Q$ and $p < 5$,

$$(Hf, f) \ge \lambda_3'(Sf, Sf) \ge \lambda_3'\lambda_2'(f, f), \tag{3.41}$$

which implies that $\mu_2 \ge \lambda_3'\lambda_2'$, i.e.,

$$\mu_2 \ge \begin{cases} \lambda_2\lambda_3 & (1 < p \le 2), \\ \lambda_2 & (2 < p < 5) \end{cases} \tag{3.42}$$

For $p > 3$, we have $L_3 \ge \lambda_2 = -(p-1)(p-5)/4$ and

$$L_3 - L_2 \ge -(p-1)(p-3)/2 =: -a. \tag{3.43}$$

Hence for any $t \in [0,1]$, we have

$$L_3 \geq tL_2 - at + (1-t)\lambda_2. \tag{3.44}$$

and so for $b > 0$, we have

$$\begin{aligned}(Hf, f) + b(f, f) &\geq (S^*(tL_2 - at + (1-t)\lambda_2)Sf, f) + b(f, f) \\ &= t\|L_1 f\|^2 - (at - (1-t)\lambda_2)(L_1 f, f) + b\|f\|^2,\end{aligned} \tag{3.45}$$

which is nonnegative if

$$b \geq (at - (1-t)\lambda_2)^2/(4t), \tag{3.46}$$

whose infimum is attained at $t = -\lambda_2/(a+\lambda_2) = (p-5)/(p-1) \in (0,1)$ for $p > 5$. Plugging this back in, we obtain the lower bound

$$\mu_1 \geq \lambda_2(a + \lambda_2) = -\frac{1}{16}(p-1)^3(p-5) \quad (p > 5). \tag{3.47}$$

We have a similar bound on μ_3 by using the even-odd decomposition $L^2(\mathbb{R}) = L^2_{ev}(\mathbb{R}) \oplus L^2_{od}(\mathbb{R})$. Let ψ_j, ξ_j be the eigenfunction of L_1 and L_3 such that

$$L_1\psi_j = \lambda_j\psi_j, \ L_3\xi_j = \lambda_j\xi_j. \tag{3.48}$$

ψ_j starts from $j = 1$ and ξ_j starts with $j = 3$. They are even for odd j and odd for even j. For any even function $f \perp Q = \psi_1$, Sf is odd and so we have $f \perp \psi_1 = Q, \psi_2$ and $Sf \perp \xi_3$. Hence by $spec(L_3)$ and $spec(L_1)$, we have

$$(Hf, f) = (L_3Sf, Sf) \geq \tilde{\lambda}_4(Sf, Sf) = \tilde{\lambda}_4(L_1 f, f) \geq \tilde{\lambda}_4\tilde{\lambda}_3(f, f), \tag{3.49}$$

where we denote

$$\tilde{\lambda}_j := \begin{cases} \lambda_j & (1 < p < p_j), \\ 1 & (p_j < p). \end{cases} \tag{3.50}$$

Thus the second eigenvalue of H on L^2_{ev} is $\geq \tilde{\lambda}_4\tilde{\lambda}_3$. Next for any odd function $f \perp \psi_2$, we have $f \perp \psi_1, \psi_2, \psi_3$. Hence we have

$$(Hf, f) = (L_3Sf, Sf) \geq \lambda'_3(Sf, Sf) = \lambda'_3(L_1 f, f) \geq \lambda'_3\tilde{\lambda}_4(f, f). \tag{3.51}$$

Similarly, every odd function $f \perp S^*\xi_3$ satisfies $f \perp \psi_1$ and $Sf \perp \xi_3, \xi_4$, so

$$(Hf, f) \geq \tilde{\lambda}_5\tilde{\lambda}_2(f, f). \tag{3.52}$$

Hence the second eigenfunction on L^2_{od} is $\geq \max(\tilde{\lambda}_4\lambda'_3, \tilde{\lambda}_5\tilde{\lambda}_2) \geq \tilde{\lambda}_4\tilde{\lambda}_3$. Therefore we have $\mu_3 \geq \tilde{\lambda}_3\tilde{\lambda}_4$, i.e.,

$$\mu_3 \geq \begin{cases} \lambda_3\lambda_4 & (1 < p < 5/3), \\ \lambda_3 & (5/3 < p < 2), \\ 1 & (2 < p). \end{cases} \tag{3.53}$$

This argument, however, does not yield any useful estimates for the higher μ_j. □

3.7 Resonance for $p = 3$

In the theory of dispersive estimates for the linear Schrödinger evolution, it is important to know whether or not the endpoints of the continuous spectrum of the linear operator are eigenvalues or *resonances*. For our $\mathcal{L}$, the endpoints are $\lambda = \pm i$. Resonance here refers to a function ϕ which satisfies the eigenvalue problem locally in space with eigenvalue i or $-i$, but which does not belong to $L^2(\mathbb{R}^n)$. For dimension $n = 1$, one requires $\phi \in L^\infty(\mathbb{R})$. (Note for comparison's sake that in one dimension, the operator $-d^2/dx^2$ has a resonance – corresponding to the constant function – at the endpoint 0 of its continuous spectrum.)

Before we made the numerical calculation, we did not expect to see any resonance. However, from Figure 1, one sees that $\kappa = \sqrt{\mu_2}$ converges to 1 as $p \to 3$. What does the point $\kappa = 1$ at $p = 3$ correspond to? A natural conjecture is that it is a resonance or an eigenvalue, since the $p = 3$ case is well-known to be completely integrable and special phenomena may occur.

This is indeed the case since we have the following solution to the eigenvalue problem (2.12) when $p = 3$,

$$\phi = \begin{bmatrix} 1 - Q^2 \\ i \end{bmatrix}, \quad \lambda = i. \tag{3.54}$$

It is clear that $\phi \in L^\infty(\mathbb{R})$ but $\phi \notin L^q(\mathbb{R})$ for any $q < \infty$.

Let $u_p(x)$ denote the real-valued (and suitably normalized) solution of (2.14) corresponding to $\mu = \mu_2$. It is the first component of the eigenfunction of (2.12). A natural question is: does $u_p(x)$ converge in some sense to $u_3(x) := 1 - Q^2(x)$ as $p \to 3$? Since $u_p - u_3$ is not in $L^q(\mathbb{R})$ for all $q \in [1, \infty)$, it seems natural to measure the convergence in the following weighted norm,

$$\|f\|_{\mathrm{w}} := \int_{\mathbb{R}} \mathrm{w}(f)^2(x)\, dx,$$

where a weighting operator w is defined by $\mathrm{w}(f)(x) := f(x)\frac{1}{\sqrt{1+x^2}}$. This de-emphasizes the value of $u_p - u_3$ for x large, and so it should converge to 0 as p goes to 3. This is confirmed numerically as follows.

Let $u_3 := 1 - Q^2$ and $\delta := \|u_3\|_{\mathrm{w}}$. In Appendix we will propose a numerical method to solve for the eigenpair $\{\lambda, [u_p(x),\ w_p(x)]^\top\}$ of (2.12) corresponding to $\mu_2 = -\lambda^2$. Renormalize $u_p(x)$ for $p \neq 3$ so that it is real-valued, $u_p(0) < 0$, and $\|u_p\|_{\mathrm{w}} = \delta$. In Figure 8(c) we plot u_3 in a large interval $|x| < 130$ with $\delta = 1.3588$. According to the numerical method in Appendix, we get $u_{2.8}, u_{2.9}, u_{3.1}$ and $u_{3.2}$ plotted in Figure 8(a), (b), (d) and (e), respectively. The vertical range is roughly $[-1, 1]$. In Figure 8(f)–(j) we plot $\mathrm{w}(u_p)$ for $p = 2.8, 2.9, 3, 3.1$ and 3.2, for $|x| < 130$ and vertical range $[-1, 0.5]$.

In Figure 9 we plot p vs. $\|u_p - u_3\|_{\mathrm{w}}$ and observe that $u_p(x)$ converge to $u_3(x)$ in the weighted norm $\|\cdot\|_{\mathrm{w}}$ as $p \to 3$. In the numerical calculation for Figure 9, our increment for p is 0.01.

Remark 3.10 For the operators L_+L_- and L_-L_+, and in general 4-th order operators, it seems difficult to exclude the possibility that $\mu = 1$ is an eigenvalue. Consider the following

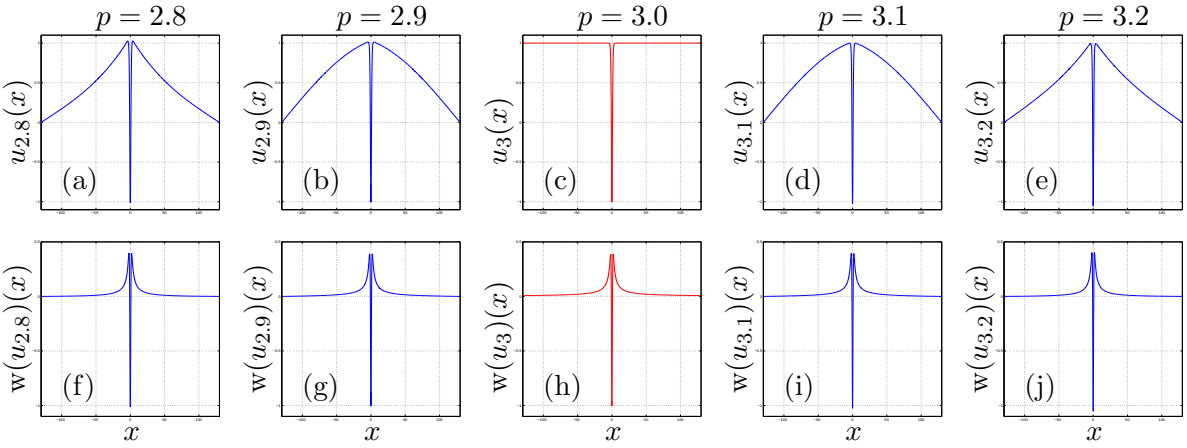

Figure 8: $u_p(x)$ & $\mathrm{w}(u_p)(x)$ for $p = 2.8, 2.9, 3, 3.1$ and 3.2.

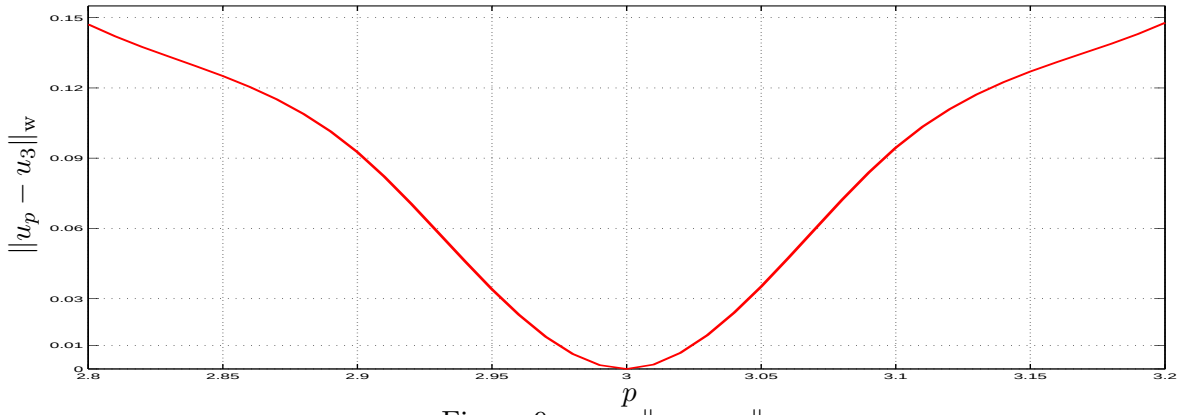

Figure 9: p vs. $\|u_p - u_3\|_{\mathrm{w}}$.

example. Let $\tilde{H} := (L_+)^2$ with $p = \sqrt{8}-1$. Note -1 is an eigenvalue of L_+ when $p = \sqrt{8}-1$. Hence 1 is an eigenvalue of $\tilde{H}$, at the endpoint of its continuous spectrum.

It would be interesting to prove the above convergence analytically and characterize the leading order behavior near $p = 3$ as we did in Theorem 2.6.

4 Excited states with angular momenta

In this section we consider excited states with angular momenta in $\mathbb{R}^n$, $n \geq 2$. Let $k = [n/2]$, the largest integer no larger than $n/2$. For $x = (x_1, \ldots, x_n) \in \mathbb{R}^n$, use polar coordinates r_j and θ_j for each pair x_{2j-1} and x_{2j}, $j = 1, \ldots, k$. P. L. Lions [20] considers solutions of the form

$$Q(x) = \phi(r_1, r_2, \ldots r_k, x_n)\, e^{i(m_1\theta_1 + \cdots m_k\theta_k)}, \qquad m_j \in \mathbb{Z}.$$

The dependence of ϕ in x_n is dropped if n is even. He proves the existence of energy minimizing solutions in each such class.

For the simplest case $n = 2$, $Q(x) = \phi(r)\, e^{im\theta}$ and, by (1.3), $\phi = \phi(r)$ satisfies

$$-\phi'' - \frac{1}{r}\phi' + \frac{m^2}{r^2}\phi + \phi - |\phi|^{p-1}\phi = 0, \quad (r > 0). \tag{4.1}$$

The natural boundary conditions are

$$\lim_{r\to 0} r^{-m}\phi(r) = \alpha, \quad \lim_{r\to 0} r^{-m+1}\phi'(r) = m\alpha, \quad \lim_{r\to\infty} \phi(r) = 0, \tag{4.2}$$

for some $\alpha \geq 0$. One can choose $\phi(r)$ real-valued. It is shown by Iaia-Warchall [16] that (4.1)–(4.2) has countably infinite many solutions, denoted by $\phi_{m,k,p}(r)$, each has exactly k positive zeros. They correspond to "m-equivariant" nonlinear bound states of the form

$$Q_{m,k,p} = \phi_{m,k,p}(r)\, e^{im\theta}, \qquad (k = 0, 1, 2, \ldots). \tag{4.3}$$

Note that $Q_{m,k,p}$ are radial if and only if $m = 0$, and the ground state $Q = Q_{0,0,p}$ is considered in the previous sections. The uniqueness question of $\phi_{m,k,p}(r)$ is not addressed in [16]. It is proved for the case $k = 0$ in [23].

Mizumachi [23]–[26] considered the stability problem for these solutions. He showed that

1. Under m-equivariant perturbations of the form $\varepsilon(r)e^{im\theta}$, $Q_{m,0,p}$ are stable for $1 < p < 3$ and unstable for $p > 3$;

2. Under general perturbations, $Q_{m,k,p}$ are unstable for $p > 3$ for any k;

3. linear (spectral) instability implies nonlinear instability; (it can be also obtained by extending the results in [30] to higher dimensions using the method of [1]);

4. For fixed $p > 1$, if $m > M(p)$ is sufficiently large, $Q_{m,k,p}$ are linearly unstable and its linearized operator has a positive eigenvalue.

We are most interested in the last result. Intuitively, for $1 < p < \infty$, $Q_{m,k,p}$ should be unstable for all $(m, k) \neq (0, 0)$ since they are excited states. Can this be observed numerically? It turns out to be true for p away from 1, but false for p near 1.

In the following, we first describe our numerical methods for $k = 0$ and next discuss their relations. We will discuss our numerical results in the end. We only compute $m = 1, 2$ but the same methods work for other m.

Remark 4.1 Our numerical methods do not apply when $k > 0$. Indeed, for $m \geq 0$ and $k > 0$, the radial functions $\phi_{m,k,p}(r)$ are sign-changing and cannot be numerically calculated using the method described in the Appendix. In fact, it is an open question whether they are unique. Assuming the uniqueness, one needs to develop a new algorithm to compute them before one can compute the spectra of $\mathcal{L}$ for $Q_{m,k,p}$.

4.1 Numerical algorithms

There are two steps in our numerical method: First, compute $\phi_{m,0,p}(r)$. Second, compute the spectra of the discretized linearized operator around $Q_{m,0,p}$. The second step is more involved and we will present three algorithms.

Step 1. Compute $\phi(r) = \phi_{m,0,p}(r)$. It is energy minimizing among all solutions of (4.1)–(4.2) for fixed m, p, and it is positive for $r > 0$. Since our algorithm in the Appendix is applicable to all positive (ground state) solutions, we can use it to calculate the discretized vector of $\phi(r)$ with a small change of the code.

Step 2. Compute the spectra of the discretized linearized operator. The linearized operator $\mathcal{L}$ has a slightly different form than (1.9) because $Q = \phi_{m,0,p}(r)e^{im\theta}$ is no longer real. With the same ansatz (1.6)–(1.7), the linearized operator $\mathcal{L}$ has the form

$$\mathcal{L}h = i\left(\Delta h - h + \frac{p+1}{2}|Q|^{p-1}h + \frac{p-1}{2}|Q|^{p-3}Q^2\bar{h}\right). \tag{4.4}$$

We have developed three algorithms for computing the spectrum of $\mathcal{L}$.

Algorithm 1. Write $Q = \phi(r)\, e^{im\theta} = \phi(r)\cos(m\theta) + i\phi(r)\sin(m\theta)$. In vector form with $\mathcal{L}$ acting on $[\operatorname{Re} h, \operatorname{Im} h]^\top$, we have

$$\mathcal{L} \sim \begin{bmatrix} 0 & -\Delta + 1 \\ \Delta - 1 & 0 \end{bmatrix} + |\phi(r)|^{p-1} \begin{bmatrix} -(p-1)\cos\sin & -\cos^2 - p\sin^2 \\ p\cos^2 + \sin^2 & (p-1)\cos\sin \end{bmatrix} (m\theta). \tag{4.5}$$

It is convenient to use polar coordinates to discretize the operator. We use a two dimensional mesh,

$$\text{2d mesh:} \quad r = 0 : \delta_r : r_{\max}, \quad \theta = 0 : \delta_\theta : 2\pi. \tag{4.6}$$

The discretized matrix has size NT by NT with $N = r_{\max}/\delta_r$ and $T = 2\pi/\delta_\theta$. We use zero boundary condition with $r_{\max} = 15$, $\delta_r = 0.04$, and $T = 160$.

Although the matrix operator (4.5) is slightly more complicated than (1.9) and the mesh is 2-dimensional, the same numerical routine can be applied to compute the spectrum of the discretized matrix of (4.5). The only difference is that the matrix size is much larger.

Algorithm 2. By restricting the problem to some invariant subspaces of $\mathcal{L}$, as we did for the computation of figures 4–5, we will reduce the problem to 1-dimension.

Observe that functions of the form $a(r)e^{ij\theta}$ with a fixed integer j are not preserved by $\mathcal{L}$ unless $j = m$, but the following L^2-subspaces are invariant under $\mathcal{L}$:

$$X_k = X_k^{(m)} = \left\{h(r,\theta) : h = a(r)e^{i(m+k)\theta} + b(r)e^{i(m-k)\theta}\right\}, \quad 0 \le j \in \mathbb{N}.$$

If $k = 0$, we drop $b(r)$ and $X_0 = \left\{h(r,\theta) : h = a(r)e^{im\theta}\right\}$. We will compute the spectra of $\mathcal{L}$ limited to each subspace X_k. Define

$$V = \frac{p-1}{2}\phi^{p-1}, \quad H_k = -\Delta_r + 1 + \frac{(m+k)^2}{r^2} - \frac{p+1}{2}\phi^{p-1}.$$

For $k = 0$, with $a = a_1 + ia_2$ and $a_1, a_2 \in \mathbb{R}$, we have

$$\mathcal{L}[a(r)e^{im\theta}] = -i\left[H_0 a - V\bar{a}\right]e^{im\theta} = [H_0(a_2 - ia_1) + V(a_2 + ia_1)]e^{im\theta}.$$

Thus, acting on $[a_1, a_2]^\top$, $\mathcal{L}|_{X_0}$ has the matrix form

$$L_{X_0} = \begin{bmatrix} 0 & H_0 + V \\ -H_0 + V & 0 \end{bmatrix}.$$

For $k > 0$, with $a = a_1 + ia_2$, $b = b_1 + ib_2$ and $a_1, a_2, b_1, b_2 \in \mathbb{R}$, we have

$$\begin{aligned}&\mathcal{L}[a(r)e^{i(m+k)\theta} + b(r)e^{i(m-k)\theta}] \\ &= [H_k(a_2 - ia_1) + V(b_2 + ib_1)]e^{i(m+k)\theta} + [H_{-k}(b_2 - ib_1) + V(a_2 + ia_1)]e^{i(m-k)\theta}.\end{aligned}$$

Thus, acting on $[a_1, a_2, b_1, b_2]^\top$, $\mathcal{L}|_{X_k}$ has the matrix form

$$L_{X_k} = \begin{bmatrix} 0 & H_k & 0 & V \\ -H_k & 0 & V & 0 \\ 0 & V & 0 & H_{-k} \\ V & 0 & -H_{-k} & 0 \end{bmatrix}.$$

To discretize the operator, we use the one-dimensional mesh

$$\text{1d mesh:} \quad r = 0 : \delta_r : r_{\max}, \quad N = r_{\max}/\delta_r. \tag{4.7}$$

The matrix corresponding to X_0 has size $2N$ by $2N$. The matrix for X_k with $k > 0$ has size $4N$ by $4N$. We use zero boundary condition with $r_{\max} = 30$ and $\delta_r = 0.01$.

Counting multiplicity, the eigenvalues of $\mathcal{L}$ is the union of eigenvalues of $\mathcal{L}|_{X_k}$ with $k = 0, 1, 2, \ldots$.

Algorithm 3. Instead of the form (1.6), include the phase $e^{im\theta}$ in the linearization: $\psi = (\phi + h)e^{im\theta + it}$. Then the linearized operator acting on $[\operatorname{Re} h, \operatorname{Im} h]^\top$ is

$$\mathcal{L}' = \begin{bmatrix} -2m/r^2\partial_\theta & -\Delta + 1 + m^2/r^2 - \phi^{p-1} \\ -(-\Delta + 1 + m^2/r^2 - p\phi^{p-1}) & -2m/r^2\partial_\theta \end{bmatrix}$$

which is invariant on subspaces $Z_k = \left\{[a_1(r), a_2(r)]^\top e^{ik\theta}\right\}$ with integers k. We have

$$\mathcal{L}' \begin{bmatrix} a_1(r) \\ a_2(r) \end{bmatrix} e^{ik\theta} = e^{ik\theta} L_{m,k} \begin{bmatrix} a_1(r) \\ a_2(r) \end{bmatrix},$$

where

$$L_{m,k} := \begin{bmatrix} -\frac{2imk}{r^2} & -\Delta_r + 1 + \frac{m^2+k^2}{r^2} - \phi^{p-1} \\ -(-\Delta_r + 1 + \frac{m^2+k^2}{r^2} - p\phi^{p-1}) & -\frac{2imk}{r^2} \end{bmatrix}$$

acting on radial functions. We use the same one-dimensional mesh (4.7) as in Algorithm 2. For every k, the matrix size is $2N$ by $2N$. We then compute the spectra of $L_{m,k}$ for each k.

Counting multiplicity, the eigenvalues of $\mathcal{L}$ is the union of eigenvalues of $L_{m,k}$ with $k = 0, \pm 1, \pm 2, \ldots$.

4.2 Properties of these algorithms

We now address the relation between these algorithms. First note that X_k is essentially the sum of Z_k and Z_{-k}. Let us make it more precise and suppose $k > 0$. The case $k = 0$ is easier. A function $h = (a_1 + ia_2)(r)e^{i(m+k)\theta} + (b_1 + ib_2)(r)e^{i(m-k)\theta}$ in $X_k \subset L^2(\mathbb{R}^2)$ can be identified with $[a_1, a_2, b_1, b_2] \in \tilde{X}_k = L^2_{rad}(\mathbb{R}^2; \mathbb{R}^4)$. The space $\tilde{X}_k$ is a subspace of $L^2_{rad}(\mathbb{R}^2; \mathbb{C}^4)$ on which we compute the spectrum. The function h can be also identified with

$$\begin{bmatrix} a_1(r) \\ a_2(r) \end{bmatrix} e^{ik\theta} + \begin{bmatrix} b_1(r) \\ b_2(r) \end{bmatrix} e^{-ik\theta},$$

the collection of which form a subspace of $Z_k \oplus Z_{-k}$ with real components.

Nullspace of $\mathcal{L}$. The nullspace of $\mathcal{L}$ gives a good test of the correctness of our numerical results. For $k = 0$, the 0-eigenfunction iQ of $\mathcal{L}$ corresponds to $[0, \phi]^\top e^{im\theta}$ in X_0 and $[0, \phi]^\top$ in Z_0. The generalized eigenfunction $Q_1 = \frac{2}{p-1}Q + x \cdot \nabla Q$ corresponds to $[Q_1, 0]^\top e^{im\theta}$ in X_0 and $[\frac{2}{p-1}\phi + r\phi', 0]^\top$ in Z_0. Since $X_0 \subset L^2(\mathbb{R}^2, \mathbb{C})$, they also provide two (generalized) eigenvectors for Algorithm 1.

For $k = \pm 1$, the 0-eigenfunctions

$$2Q_{x_1} = 2(\phi' \cos\theta - i\psi \sin\theta)e^{im\theta} = (\phi' - \psi)e^{i(m+1)\theta} + (\phi' + \psi)e^{i(m-1)\theta},$$

$$2Q_{x_2} = 2(\phi' \sin\theta + i\psi \cos\theta)e^{im\theta} = i(-\phi' + \psi)e^{i(m+1)\theta} + i(\phi' + \psi)e^{i(m-1)\theta},$$

where $\psi = m\phi/r$, belong to X_1, and correspond to 0-eigenvectors $[\phi' - \psi, 0, \phi' + \psi, 0]^\top$ and $[0, -\phi' + \psi, 0, \phi' + \psi]^\top$ of L_{X_1}. For Algorithm 3, they correspond to the following vectors in $Z_1 \oplus Z_{-1}$,

$$2\begin{bmatrix} \phi' \cos\theta \\ -\psi \sin\theta \end{bmatrix} = W_+ e^{i\theta} + W_- e^{-i\theta}, \quad 2\begin{bmatrix} \phi' \sin\theta \\ \psi \cos\theta \end{bmatrix} = -iW_+ e^{i\theta} + iW_- e^{-i\theta}$$

where

$$W_\pm = \begin{bmatrix} \phi' \\ \pm i\psi \end{bmatrix}, \quad L_{m,\pm 1} W_\pm = \begin{bmatrix} 0 \\ 0 \end{bmatrix}.$$

Thus $W_+ e^{i\theta}$ is a 0-eigenvector of $\mathcal{L}'$ in Z_1, and $W_- e^{-i\theta}$ is a 0-eigenvector of $\mathcal{L}'$ in Z_{-1}.

The generalized eigenfunctions

$$ix_1 Q = ir\phi \cos\theta e^{im\theta} = ir\phi e^{i(m+1)\theta} + ir\phi e^{i(m-1)\theta}$$

$$ix_2 Q = ir\phi \sin\theta e^{im\theta} = r\phi e^{i(m+1)\theta} - r\phi e^{i(m-1)\theta}$$

also lie in X_1 and correspond to generalized 0-eigenvectors $[0, r\phi, 0, r\phi]^\top$ and $[r\phi, 0, -r\phi, 0]^\top$ of L_{X_1}. For Algorithm 3, they correspond to $[0, r\phi\cos\theta]^\top$ and $[0, r\phi\sin\theta]^\top$ in $Z_1 \oplus Z_{-1}$. By the same consideration as for Q_{x_1} and Q_{x_2}, their span over $\mathbb{C}$ is the same as the span of $[0, r\phi]^\top e^{i\theta} \in Z_1$ and $[0, r\phi]^\top e^{-i\theta} \in Z_{-1}$. One can check that

$$L_{m,\pm 1}\begin{bmatrix} 0 \\ r\phi \end{bmatrix} = -2\begin{bmatrix} \phi' \\ \pm i\psi \end{bmatrix}. \tag{4.8}$$

Thus, the multiplicity of 0-eigenvalue in each of X_0, Z_{-1}, Z_0 and Z_1 is at least 2. The multiplicity of 0-eigenvalue on X_1 is at least 4.

Symmetry of spectra. If

$$L_{m,k}\begin{bmatrix}A\\B\end{bmatrix} = \lambda\begin{bmatrix}A\\B\end{bmatrix}$$

then

$$L_{m,-k}\begin{bmatrix}\bar{A}\\\bar{B}\end{bmatrix} = \bar{\lambda}\begin{bmatrix}\bar{A}\\\bar{B}\end{bmatrix}, \quad L_{m,-k}\begin{bmatrix}A\\-B\end{bmatrix} = -\lambda\begin{bmatrix}A\\-B\end{bmatrix}, \quad L_{m,k}\begin{bmatrix}\bar{A}\\-\bar{B}\end{bmatrix} = -\bar{\lambda}\begin{bmatrix}\bar{A}\\-\bar{B}\end{bmatrix}.$$

In particular, if $\lambda \in \sigma(L_{m,k})$, then $-\bar{\lambda} \in \sigma(L_{m,k})$, and $\bar{\lambda}, -\lambda \in \sigma(L_{m,-k})$. Thus $\sigma(L_{m,k})$ itself is symmetric w.r.t. the imaginary axis, and $\sigma(L_{m,k})$ and $\sigma(L_{m,-k})$ are symmetric w.r.t. the real axis.

Similarly, one can show that the spectra of L_{X_k} are symmetric with respect to both real and imaginary axes.

Equivalence of Algorithms 2 and 3. In Algorithm 2, for $k > 0$, we can write

$$L_{X_k} = \begin{bmatrix}H_k J & VU\\ VU & H_{-k}J\end{bmatrix}$$

where

$$J = \begin{bmatrix}0 & 1\\-1 & 0\end{bmatrix}, \quad U = \begin{bmatrix}0 & 1\\1 & 0\end{bmatrix}, \quad I = \begin{bmatrix}1 & 0\\0 & 1\end{bmatrix}.$$

Let

$$M = \begin{bmatrix}I & -J\\I & J\end{bmatrix}, \quad M^{-1} = \frac{1}{2}\begin{bmatrix}I & I\\J & -J\end{bmatrix}, \quad P = \begin{bmatrix}1 & 0 & 0 & 0\\0 & 0 & 1 & 0\\0 & 1 & 0 & 0\\0 & 0 & 0 & 1\end{bmatrix}, \quad P^{-1} = P.$$

Noting $JU = -UJ$, we have

$$M^{-1}L_{X_k}M = \begin{bmatrix}\alpha J + cU & -\beta\\ -\beta & \alpha J + cU\end{bmatrix} = \begin{bmatrix}0 & \alpha+c & \beta & 0\\ -\alpha+c & 0 & 0 & \beta\\ -\beta & 0 & 0 & \alpha+c\\ 0 & -\beta & -\alpha+c & 0\end{bmatrix}$$

where

$$\alpha = \frac{1}{2}(H_k + H_{-k}) = H_0 + \frac{k^2}{r^2}, \quad \beta = \frac{1}{2}(H_k - H_{-k}) = \frac{2mk}{r^2}, \quad c = V.$$

Let

$$L' := P^{-1}M^{-1}L_{X_k}MP = \begin{bmatrix}0 & \beta & \alpha+c & 0\\ -\beta & 0 & 0 & \alpha+c\\ -\alpha+c & 0 & 0 & \beta\\ 0 & -\alpha+c & -\beta & 0\end{bmatrix}.$$

In Algorithm 3, $L_{m,k}$ acts on $[A(r), B(r)]^\top$. If we write the enlarged matrix of $L_{m,k}$ acting on $[\operatorname{Re} A, \operatorname{Im} A, \operatorname{Re} B, \operatorname{Im} B]^\top$, the matrix is exactly L'. The matrix for $L_{m,-k}$ will be also L' if it acts on $[\operatorname{Re} A, -\operatorname{Im} A, \operatorname{Re} B, -\operatorname{Im} B]^\top$. This amounts to a choice of assigning J or $-J$ to the complexification of i.

More precisely, if $L_{m,k}u = \lambda u$ with $u = [A, B]^\top$, then $L_{m,k}iu = \lambda iu$. Write $A = A_1 + iA_2$ and $B = B_1 + iB_2$ and suppose $k > 0$. These two equations are equivalent to

$$L' \begin{bmatrix} A_1 \\ A_2 \\ B_1 \\ B_2 \end{bmatrix} = \begin{bmatrix} \operatorname{Re} \lambda A \\ \operatorname{Im} \lambda A \\ \operatorname{Re} \lambda B \\ \operatorname{Im} \lambda B \end{bmatrix}, \qquad L' \begin{bmatrix} -A_2 \\ A_1 \\ -B_2 \\ B_1 \end{bmatrix} = \begin{bmatrix} -\operatorname{Im} \lambda A \\ \operatorname{Re} \lambda A \\ -\operatorname{Im} \lambda B \\ \operatorname{Re} \lambda B \end{bmatrix}.$$

Adding the second equation multiplied by $-i$ to the first equation, we get

$$L'w = \lambda w, \quad w = [A, -iA, B, -iB]^\top.$$

Taking conjugation we get $L'\bar{w} = \bar{\lambda}\bar{w}$. Thus λ and $\bar{\lambda}$ are eigenvalues of L', and hence of L_{X_k}. Since $L_{m,k}u = \lambda u$ iff $L_{m,-k}\bar{u} = \bar{\lambda}\bar{u}$, eigenvalues of $L_{m,-k}$ also correspond to eigenvalues of L_{X_k}.

Counting eigenvalues. L_{X_k} acts on $L^2_{rad}(\mathbb{R}^2, \mathbb{C}^4)$ while $L_{m,\pm k}$ act on $L^2_{rad}(\mathbb{R}^2, \mathbb{C}^2)$. The eigenvalues of L_{X_k} is the union of eigenvalues of $L_{m,k}$ and $L_{m,-k}$. For any ball B_R on the complex plane disjoint from the continuous spectrum $\Sigma_c = \{ir : r \in \mathbb{R}, |r| \geq 1\}$,

$$\#(\sigma(L_{X_k}) \cap B_R) = \#(\sigma(L_{m,k}) \cap B_R) + \#(\sigma(L_{m,-k})) \cap B_R$$

which is equal to $2\#(\sigma(L_{m,k}) \cap B_R)$ if the center of B_R is on the real axis.

Numerical efficiency. Algorithm 1 is 2-dimensional, and thus more expensive to compute and less accurate. Both Algorithms 2 and 3 are one-dimensional and more accurate.

The benefit of Algorithm 3 than Algorithm 2 is that it further decomposes the subspace of $L^2(\mathbb{R}^2, \mathbb{C}^4)$ corresponding to X_k to two subspaces. Although its matrix size is only half that of Algorithm 2, its components are complex and hence require more storage space. Numerically these two algorithms are not very different.

4.3 Numerical results

The results of our numerical computations of the spectra of $\mathcal{L}$ for $m = 1, 2$ and various k and p are shown in Figures 10–15. As before, we focus on eigenvalues in the square $\{a + bi : |a| < 1, |b| < 1\}$. Purely imaginary eigenvalues with modulus greater than 1 correspond to the continuous spectrum of $\mathcal{L}$, and are discrete due to discretization.

Let us first describe some simple observations:

1. The distribution of eigenvalues, see Figures 10–11, is more complicated and interesting than Figures 1–5. There are not only purely imaginary eigenvalues and real eigenvalues but also complex eigenvalues, whose existence implies instability.

2. In Figures 12–13, we compare the results obtained from three algorithms. For Algorithms 2 and 3 the parameter k ranges from 0 to 9. Results from these algorithms have high degree of agreement, except when p near 3 and eigenvalues near 0. We will discuss this exceptional case in the end.

3. For Algorithms 2 and 3, the numerical 0-eigenvalue occurs only when $k = 0$ and $k = \pm 1$. It agrees with our discussion in the previous subsection. Their multiplicities also match and there is no unaccounted eigenvector. In particular, $N_g(\mathcal{L})$ has dimension 6 if $p \neq 3$ and 8 if $p = 3$, the same as the case of ground states. We also numerically verified the nullspace, for example, the discrete version of (4.8) is correct.

4. As p increases, two pairs of purely imaginary eigenvalues may collide away from 0, and then split to a quadruple of complex eigenvalues which are neither real nor purely imaginary. For $m = 1$, this bifurcation phenomenon appears three times before $p = 1.55$ and there are 3 complex quadruples for $p > 1.55$. For $m = 2$, it occurs five times before $p = 1.5$ and there are 5 quadruples for $p > 1.5$. These complex eigenvalues seem to move away from the imaginary axis as p increases further.

5. As p increases to 3, (by Algorithms 2 and 3), a pair of purely imaginary eigenvalues from 0-th subspace collide at 0 and then split to a pair of real eigenvalues as p increases further. This is the same picture as in the ground state case in section 3. Indeed, Mizumachi [23] proves that $Q_{m,0,p}$ are stable in the 0-th subspace if $p < 3$ and unstable if $p > 3$. Thus $p = 3$ is a bifurcation point. Also note that when $p = 3$ the NLS (1.1) has conformal invariance and explicit blow-up solutions can be found as in the ground state case.

6. In Figures 14–15 we observe the bifurcation more closely. For $m = 1$, the bifurcation occurs when (k, p, λ) equal

$$(0,\, 3,\, 0), \quad (1,\, 1.52765\, -0.436i), \quad (2,\, 1.0165,\, -0.016i), \quad (3,\, 1.3495,\, -0.219i).$$

   For $m = 2$, the bifurcation occurs when (k, p, λ) equal

$$(0,\, 3,\, 0), \quad (1,\, 1.357,\, -0.180i), \quad (2,\, 1.007,\, -0.027i), \quad (3,\, 1.0245,\, -0.035i)$$

   and

$$(4,\, 1.0455,\, -0.045i), \quad (5,\, 1.3955,\, -0.347i).$$

7. Due to the existence of complex eigenvalues for $m = 1, 2$ and $p \geq 1.02$, $Q_{m,0,p}$ is spectrally unstable for these parameters. However, all these complex eigenvalues bifurcate from some discrete eigenvalues $\pm bi$ with $|b| < 1$ and $p > 1.008$. Our computation for both $m = 1, 2$ and

$$p = \ell \cdot 0.001, \quad \ell = 1, 2, 3, \ldots, 8, \quad \text{(up to 15 if } m = 1)$$

does not find any complex eigenvalues. This suggests that the two excited states $\phi_{1,0,p}(r)e^{i\theta}$ and $\phi_{2,0,p}(r)e^{i2\theta}$ are *linearly stable* when p is sufficiently close to 1. It is possible that the numerical error increases enormously as $p \to 1_+$ due to the artificial boundary condition, since the spectrum is approaching to the continuous one for $p = 1$. This has to be verified analytically in the future.

We finally discuss the exceptional case when p is near 3 for eigenvalues near 0. In this case Algorithm 1 produces an quadruple of complex eigenvalues $\pm 0.0849 \pm 0.0836i$, and the 0-eigenvalue has multiplicity 4. We expect to see larger errors from Algorithm 1 but the error in this exceptional case is much larger. It is related to the large size of a Jordon block for the 0 eigenvalue. As discussed in the previous subsection, the nullspace is at least 6 dimensional. The analysis in section 2.3 suggests that (we do not claim a proof), as p goes to the bifurcation exponent $p_c = 3$ from below, a pair of imaginary eigenvalues merges into the Jordon block containing the eigenfunctions iQ and Q_1, and the Jordon block becomes size 4. As is well-known in matrix analysis (see [9, p.324], [41]), if a matrix contains a Jordon block of size ℓ, the computed eigenvalues corresponding to that block have errors of order $\varepsilon^{1/\ell}$, where ε is the sum of the machine zero, the truncation error from discretization, and the perturbation (from varying p). Since $\delta_r = 0.04$ for Algorithm 1 and the truncation error of a central difference scheme for Δ_r has order $O(\delta_r^2)$, the error for the zero eigenvalue near $p = 3$ could be

$$(\delta_r^2)^{1/4} \approx 0.2.$$

In contrast, for other bifurcation points on the imaginary axis, the Jordon block at the bifurcation exponent is of size 2 and the error is of order $(\delta_r^2)^{1/2} = 0.04$. In practice, the error is smaller due to cancellation and the numerical results by Algorithm 1 do not differ too much from those by Algorithms 2 and 3. Also note that numerically the 0 eigenspace has dimension 4, accounting for Q_{x_j} and ix_jQ. The complex quadruple correspond to iQ, Q_1 and the joining pair of nonzero eigenvalues.

Appendix: Numerical method

In this section we describe a numerical method to compute the spectrum of the linear operator $\mathcal{L}$ defined by (1.8) for $p > 1$ and space dimension $n \geq 1$. There are two main steps in this method. First, we will solve the nonlinear problem (1.3) for Q: we will discretize it into a nonlinear algebraic equation, and then solve it by an iterative method. Second, we will compute the spectrum of $\mathcal{L}$: we will discretize the operator $\mathcal{L}$ into a large-scale linear algebraic eigenvalue problem and then use implicitly restarted Arnoldi methods to deal with this problem.

Hereafter, we use the bold face letters or symbols to denote a matrix or a vector. For $\mathbf{A} \in \mathbb{R}^{M\times N}$, $\mathbf{q} = (q_1, \ldots, q_N)^\top \in \mathbb{R}^N$, $\mathbf{q}^{\circledcirc} = \mathbf{q} \circ \cdots \circ \mathbf{q}$ denotes the p-time Hadamard product of $\mathbf{q}$, and $[\![\mathbf{q}]\!] := \mathrm{diag}(\mathbf{q})$ the diagonal matrix of $\mathbf{q}$.

Step I. We first discretize equation (1.3) into a nonlinear algebraic equation and consider it on an n-dimensional ball $\Omega = \{x \in \mathbb{R}^n : |x| \leq R, R \in \mathbb{R}\}$. We rewrite the Laplace

operator $-\Delta$ in the polar coordinate system with a Dirichlet boundary condition. Based on the recently proposed discretization scheme [19], the *standard central finite difference method*, we discretize $-\Delta\mathbf{q}(x)$ into

$$\mathbf{A}\mathbf{q} = \mathbf{A}[q_1, \ldots, q_N]^\top,\ \mathbf{A} \in \mathbb{R}^{N\times N}, \tag{A.1}$$

where $\mathbf{q}$ is an approximation of the function $Q(x)$. The matrix $\mathbf{A}$ is irreducible and diagonally-dominant with positive diagonal entries. The discretization of the nonlinear equation (1.3) can now be formulated as the following nonlinear algebraic equation,

$$\mathbf{A}\mathbf{q} + \mathbf{q} - \mathbf{q}^{\circledcirc} = 0. \tag{A.2}$$

We introduce an iterative algorithm [15] to solve (A.2):

$$\mathbf{A}\widetilde{\mathbf{q}}_{j+1} + \widetilde{\mathbf{q}}_{j+1} = \mathbf{q}_j^{\circledcirc}, \tag{A.3}$$

where $\widetilde{\mathbf{q}}_{j+1}$ and $\mathbf{q}_j$ are the unknown and known discrete values of the function $Q(\mathbf{x})$, respectively. The iterative algorithm is shown below.

Iterative Algorithm for Solving $Q(\mathbf{x})$.

Step 0 Let $j = 0$.
Choose an initial solution $\widetilde{\mathbf{q}}_0 > 0$ and let $\mathbf{q}_0 = \frac{\widetilde{\mathbf{q}}_0}{\|\widetilde{\mathbf{q}}_0\|_2}$.

Step 1 Solve the equation (A.3), then obtain $\widetilde{\mathbf{q}}_{j+1}$.

Step 2 Let $\alpha_{j+1} = \frac{1}{\|\widetilde{\mathbf{q}}_{j+1}\|_2}$ and normalize $\widetilde{\mathbf{q}}_{j+1}$ to obtain $\mathbf{q}_{j+1} = \alpha_{j+1}\widetilde{\mathbf{q}}_{j+1}$.

Step 3 If (convergent) then
    Output the scaled solution $(\alpha_{j+1})^{\frac{1}{p-1}}\mathbf{q}_{j+1}$. Stop.
else
    Let $j := j + 1$.
    Goto Step 1.
end

If the components of $\mathbf{q}_0$ are nonnegative, this property is preserved by each iteration $\mathbf{q}_j$, and hence also by the limit vector if it exists (see [15, Theorem 3.1]). The convergence of a subsequence of this iteration method to a nonzero vector is proved in [15, Theorem 2.1]. Although the convergence of the entire sequence is not proved, it is observed numerically to be very robust. See Chen-Zhou-Ni [5] for a survey on numerically solving nonlinear elliptic equations.

Step II. Next we discretize the operator $\mathcal{L}$ of (1.10) into a linear algebraic eigenvalue problem:

$$\mathbf{L}\begin{bmatrix} \mathbf{u} \\ \mathbf{w} \end{bmatrix} = \lambda \begin{bmatrix} \mathbf{u} \\ \mathbf{w} \end{bmatrix}, \tag{A.4}$$

where

$$\mathbf{L} = \begin{bmatrix} 0 & \mathbf{A} + \mathrm{I} - [\![\mathbf{q}^{\gamma}]\!] \\ -\mathbf{A} - \mathrm{I} + [\![p\,\mathbf{q}^{\gamma}]\!] & 0 \end{bmatrix},$$

$\gamma = p - 1$, $\mathbf{u} = (u_1, \ldots, u_N)^\top \in \mathbb{R}^N$, $\mathbf{w} = (w_1, \ldots, w_N)^\top \in \mathbb{R}^N$, and $\mathbf{q}$ is the output of the previous step, and satisfies the equation in (A.2). We use ARPACK [21] in MATLAB version 6.5 to deal with the linear algebraic eigenvalue problem (A.4) and obtain eigenvalues λ of $\mathbf{L}$ near the origin for $p > 1$ and space dimension $n \geq 1$. Furthermore, the eigenvectors of $\mathbf{L}$ can be also produced.

The Step II above can in principle be used to compute all eigenfunctions in $L^2(\mathbb{R}^n)$. However, in producing Figures 2–5, we look for eigenfunctions of the form $\phi(r)e^{im\theta}$. These problems can be reformulated as 1-D eigenvalue problems for $\phi(r)$, which can be computed using the same algorithm and MATLAB code. This dimensional reduction saves a lot of computation time and memory. Even with this dimensional reduction, and applying an algorithm for sparse matrices, the computation is still very heavy, and we cannot compute all eigenvalues in one step. We can only compute a portion of them each time.

Acknowledgments

Special thanks go to Wen-Wei Lin, whose constant advice and interest were indispensable for this project. We thank V.S. Buslaev, Y. Martel, F. Merle, T. Mizumachi, C. Sulem, and W.C. Wang for fruitful discussions and providing many references to us. We also thank the referees for many valuable suggestions. Part of the work was done when Nakanishi was visiting the University of British Columbia, Vancouver, and when Tsai was visiting the National Center for Theoretical Sciences, Hsinchu & Taipei. The hospitality of these institutions are gratefully acknowledged. The research of Chang is partly supported by National Science Council in Taiwan. The research of Gustafson and Tsai is partly supported by NSERC grants. The research of Nakanishi is partly supported by the JSPS grant no. 15740086.

References

[1] L. Almeida and Y. Guo, Dynamical instability of symmetric vortices. Rev. Mat. Iberoamericana 17 (2001), no. 2, 409–419.

[2] H. Berestycki, and P.-L. Lions, Nonlinear scalar field equations I and II. *Arch. Rat. Mech. Anal.* **82** (1983) 313-375.

[3] V. S. Buslaev and V. E. Grikurov, Simulation of Instability of bright solitons for NLS with saturating nonlinearity, *IMACS Journal Math. and Computers in Simulation* **56** (2001), no. 6, pp. 539–546.

[4] T. Cazenave, *Semilinear Schrödinger equations*, Amer. Math. Soc., 2003.

[5] G. Chen, J. Zhou, and W.-M. Ni, Algorithms and visualization for solutions of nonlinear elliptic equations. *Internat. J. Bifur. Chaos Appl. Sci. Engrg.* **10** (2000), no. 7, 1565–1612.

[6] A. Comech and D. Pelinovsky, "Purely nonlinear instability of standing waves with minimal energy", Comm. Pure Appl. Math. **56** (2003), 1565–1607.

[7] S. Cuccagna, D. Pelinovsky and V. Vougalter, Spectra of positive and negative energies in the linearized NLS problem, *Comm. Pure Appl. Math.* **58** (2005), no. 1, 1–29.

[8] L. Demanet and W. Schlag, Numerical verification of a gap condition for linearized NLS, preprint, http://www.arxiv.org/math.AP/0508235

[9] G. H. Golub and C. F. Van Loan, Matrix Computations, 3ed., John Hopkins Univ. Press, 1996.

[10] V. E. Grikurov, Perturbation of instable solitons for Generalized NLS with saturating nonlinearity, preprint, http://math.nw.ru/∼grikurov/publlist.html/proc_DD97.ps.gz

[11] M. Grillakis, Linearized instability for nonlinear Schrödinger and Klein-Gordon equations. *Comm. Pure Appl. Math.* **41** (1988), no. 6, 747–774.

[12] M. Grillakis, J. Shatah and W. Strauss, Stability theory of solitary waves in the presence of symmetry I, *J. Funct. Anal.* **74** (1987), no. 1, 160–197.

[13] S. Gustafson, K. Nakanishi and T.-P. Tsai, Asymptotic stability and completeness in the energy space for nonlinear Schrödinger equations with small solitary waves, *Int. Math. Res. Not.* **2004** (2004) no. 66, 3559–3584.

[14] J. Fröhlich, S. Gustafson, L. Jonsson, and I.M. Sigal, Solitary wave dynamics in an external potential. *Comm. Math. Phys.* **250** (2004) 613-642.

[15] T. M. Hwang and W. Wang, Analyzing and Visualizing A Discretized Semilinear Elliptic Problem with Neumann Boundary Conditions, *Numerical Methods for Partial Differential Equations* **18** (2002), pp. 261–279.

[16] Iaia, Joseph; Warchall, Henry: Nonradial solutions of a semilinear elliptic equation in two dimensions. J. Differential Equations **119** (1995), no. 2, 533–558.

[17] E. Kirr and A. Zarnescu, On the asymptotic stability of bound states in 2D cubic Schroedinger equation, preprint, http://arxiv.org/abs/math.AP/0603550

[18] M. K. Kwong, Uniqueness of positive solutions of $\Delta u - u + u^p = 0$ in $\mathbb{R}^n$, *Arch. Rat. Mech. Anal.* **105** (1989), 243–266.

[19] M.-C. Lai, A note on finite difference discretizations for poisson equation on a disk, *Numerical Methods for Partial Differential Equations* 17 (2001) no. 3, 199–203.

[20] Lions, Pierre-Louis: Solutions complexes d'équations elliptiques semilinéaires dans R^N. C. R. Acad. Sci. Paris Sér. I Math. 302 (1986), no. 19, 673–676.

[21] R.B. Lehoucq, , D.C. Sorensen and C. Yang, *ARPACK Users' Guide: Solution of Large-Scale Eigenvalue Problems with Implicitly Restarted Arnoldi Methods*, SIAM Publications, Philadelphia, 1998.

[22] Matveev, V. B. and Salle, M. A., *Darboux transformations and solitons*. Springer Series in Nonlinear Dynamics. Springer-Verlag, Berlin, 1991. x+120pp.

[23] T. Mizumachi, Vortex solitons for 2D focusing nonlinear Schrödinger equation. Differential Integral Equations 18 (2005), no. 4, 431–450.

[24] T. Mizumachi, Instability of bound states for 2D nonlinear Schrödinger equations, Discrete and continuous dynamical systems 13 (2005), No.2, 413–428.

[25] T. Mizumachi, A remark on linearly unstable standing wave solutions to NLS, Nonlinear analysis, to appear.

[26] T. Mizumachi, Instability of vortex solitons for 2D focusing NLS, Advances in Differential Equations, to appear.

[27] S.I. Pohozaev, Eigenfunctions of the equation $\Delta u + \lambda f(u) = 0$. *Sov. Math. Doklady* **5** (1965) 1408-1411.

[28] I. Rodnianski, W. Schlag, A. Soffer: Dispersive analysis of charge transfer models, *Comm. Pure Appl. Math.* 58 (2005), no. 2, 149–216.

[29] I. Rodnianski, W. Schlag, A. Soffer: Asymptotic stability of N-soliton states of NLS, preprint, http://arxiv.org/abs/math.AP/0309114

[30] J. Shatah and W. Strauss, Spectral condition for instability. Nonlinear PDE's, dynamics and continuum physics (South Hadley, MA, 1998), 189–198, Contemp. Math., 255, Amer. Math. Soc., Providence, RI, 2000.

[31] W. Schlag, Stable manifolds for an orbitally unstable NLS, preprint, http://arxiv.org/abs/math.AP/0405435

[32] W. Strauss, Existence of solitary waves in higher dimensions, *Comm. Math. Phys.* **55** (1977), 149–162.

[33] W. Strauss, *Nonlinear wave equations*, Amer. Math. Soc., 1989.

[34] C. Sulem and P.-L. Sulem, *The nonlinear Schrödinger equations: self-focusing and wave collapse*, Springer, 1999.

[35] E. C. Titchmarsh, *Eigenfunction expansions associated with second-order differential equations*, part I, 2nd ed., Oxford, 1962.

[36] T.-P. Tsai and H.-T. Yau, Asymptotic dynamics of nonlinear Schroedinger equations: resonance dominated and dispersion dominated solutions, *Comm. Pure Appl. Math.* **55** (2002) 0153–0216.

[37] T.-P. Tsai and H.-T. Yau, Stable directions for excited states of nonlinear Schrödinger equations, *Comm. Partial Diff. Equ.* **27** (2002), no. 11&12, 2363–2402.

[38] M. I. Weinstein, Nonlinear Schrödinger equations and sharp interpolation estimates. *Comm. Math. Phys.* **87** (1982/83), no. 4, 567–576.

[39] M. I. Weinstein, Modulational stability of ground states of nonlinear Schrödinger equations, *SIAM J. Math. Anal.* **16** (1985), no. 3, 472–491.

[40] M. I. Weinstein, Lyapunov stability of ground states of nonlinear dispersive evolution equations, *Comm. Pure Appl. Math.* **39** (1986), 51–68.

[41] J. H. Wilkinson, Convergence of the LR, QR, and related algorithms, *Comp. J.* **8** (1965) 77–84.

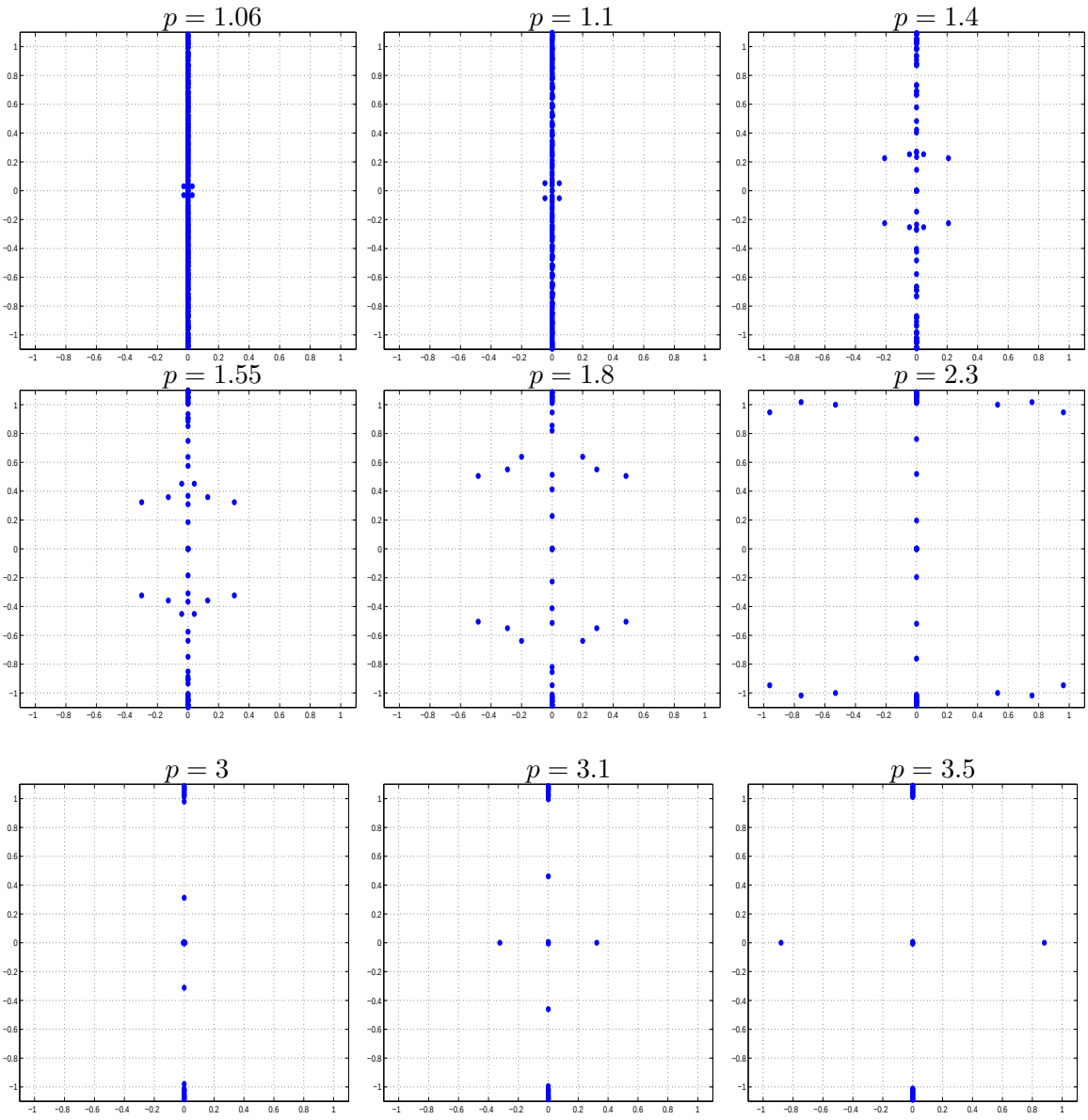

Figure 10: Spectra of $\mathcal{L}$ in $\mathbb{R}^2$ for $m = 1$ and $0 \leq k \leq 24$ as $p = 1.06, 1.1, 1.4, 1.55, 1.8, 2.3, 3, 3.1, 3.5$ computed by Algorithm 3.

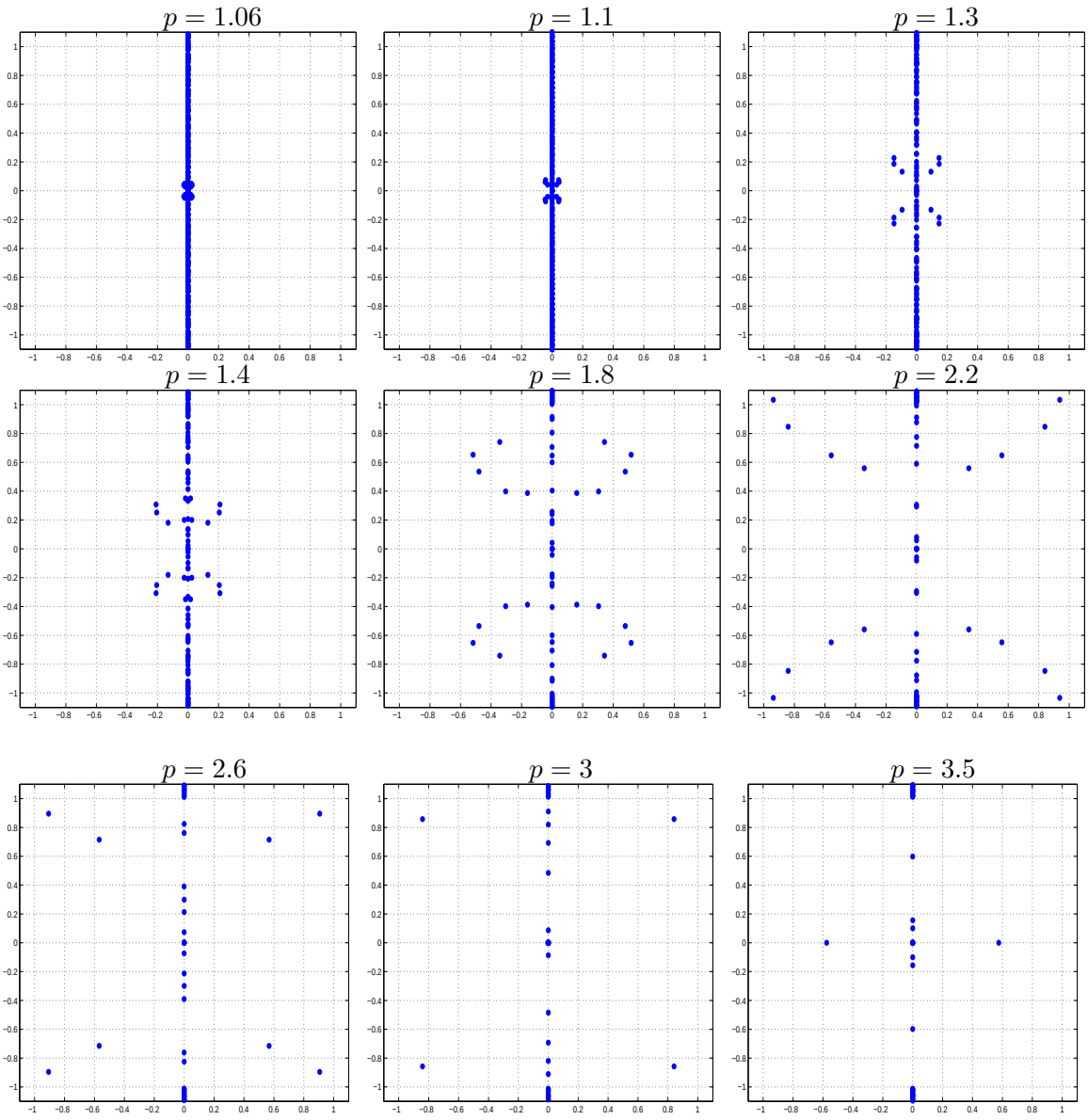

Figure 11: Spectra of $\mathcal{L}$ in $\mathbb{R}^2$ for $m = 2$ and $0 \leq k \leq 28$ as $p = 1.06, 1.1, 1.3, 1.4, 1.8, 2.2, 2.6, 3, 3.5$ computed by Algorithm 3.

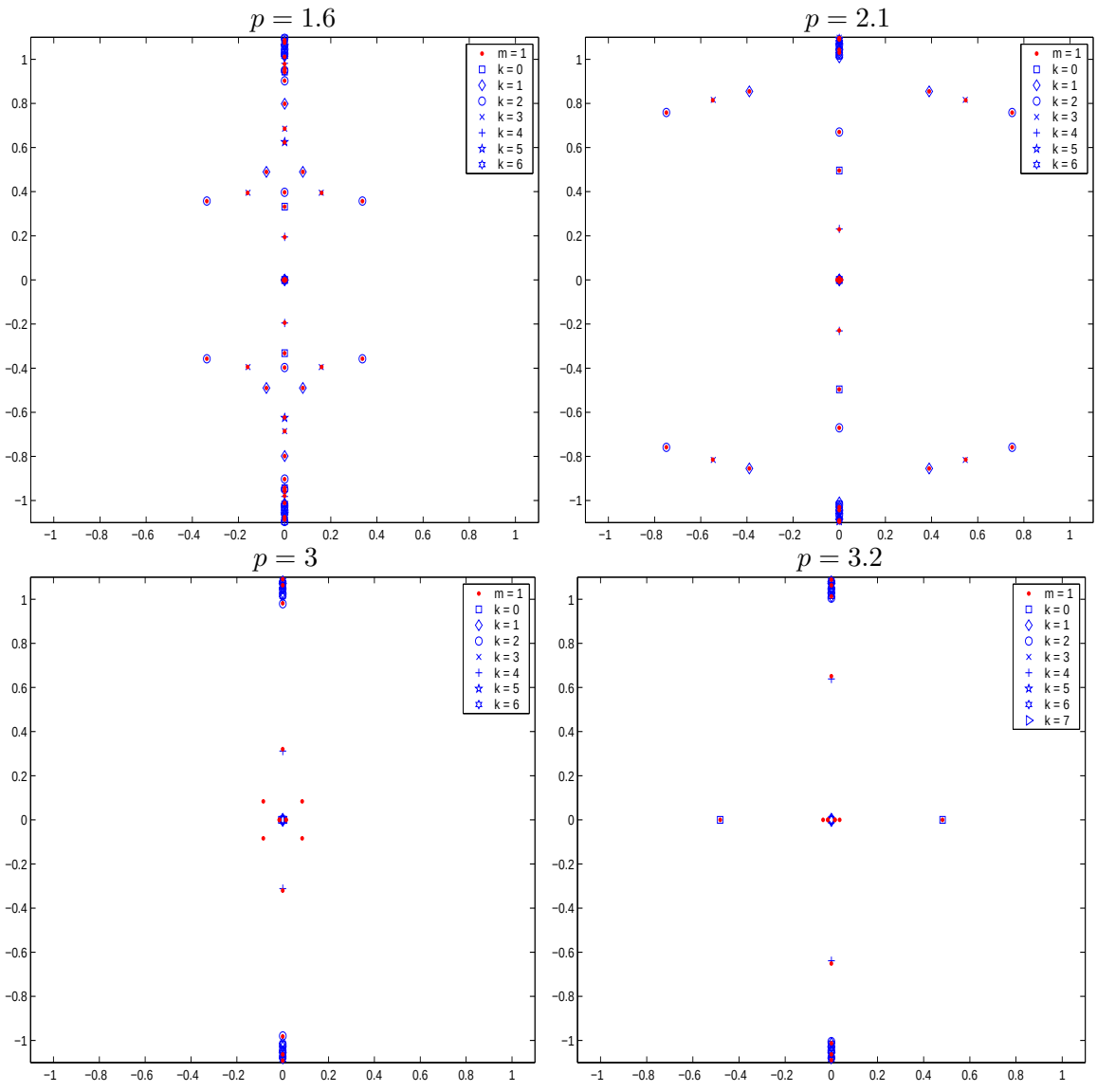

Figure 12: Spectra of $\mathcal{L}$ in $\mathbb{R}^2$ for $m = 1$ and various $p = 1.6, 2.1, 3, 3.2$. Point "$\cdot$" denotes the spectra computed by Algorithm 1 and the others symbols denote the spectra computed by Algorithms 2 and 3.

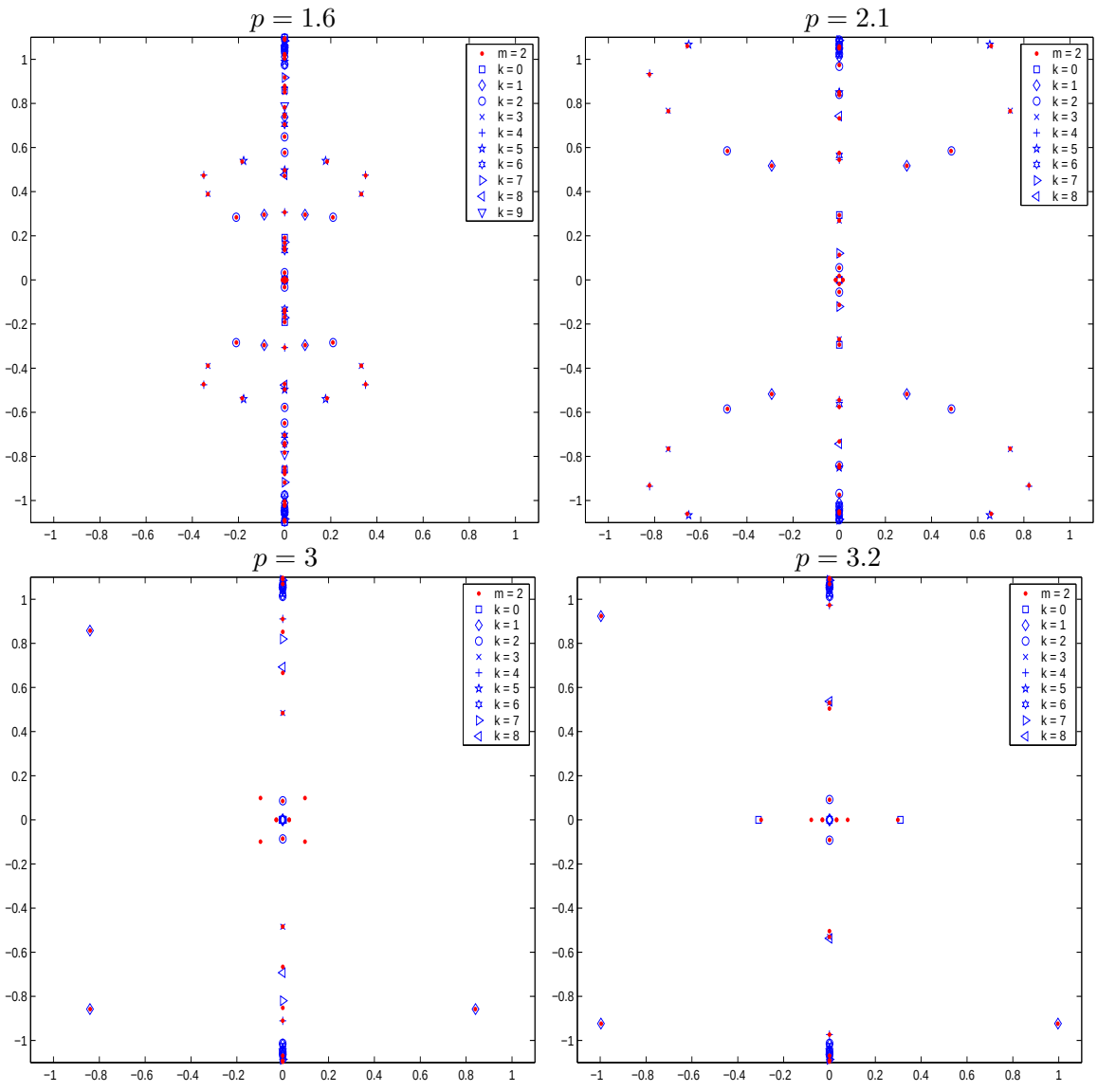

Figure 13: Spectra of $\mathcal{L}$ in $\mathbb{R}^2$ for $m = 2$ and various $p = 1.6, 2.1, 3, 3.2$. Point "$\cdot$" denotes the spectra computed by Algorithm 1 and the others symbols denote the spectra computed by Algorithms 2 and 3.

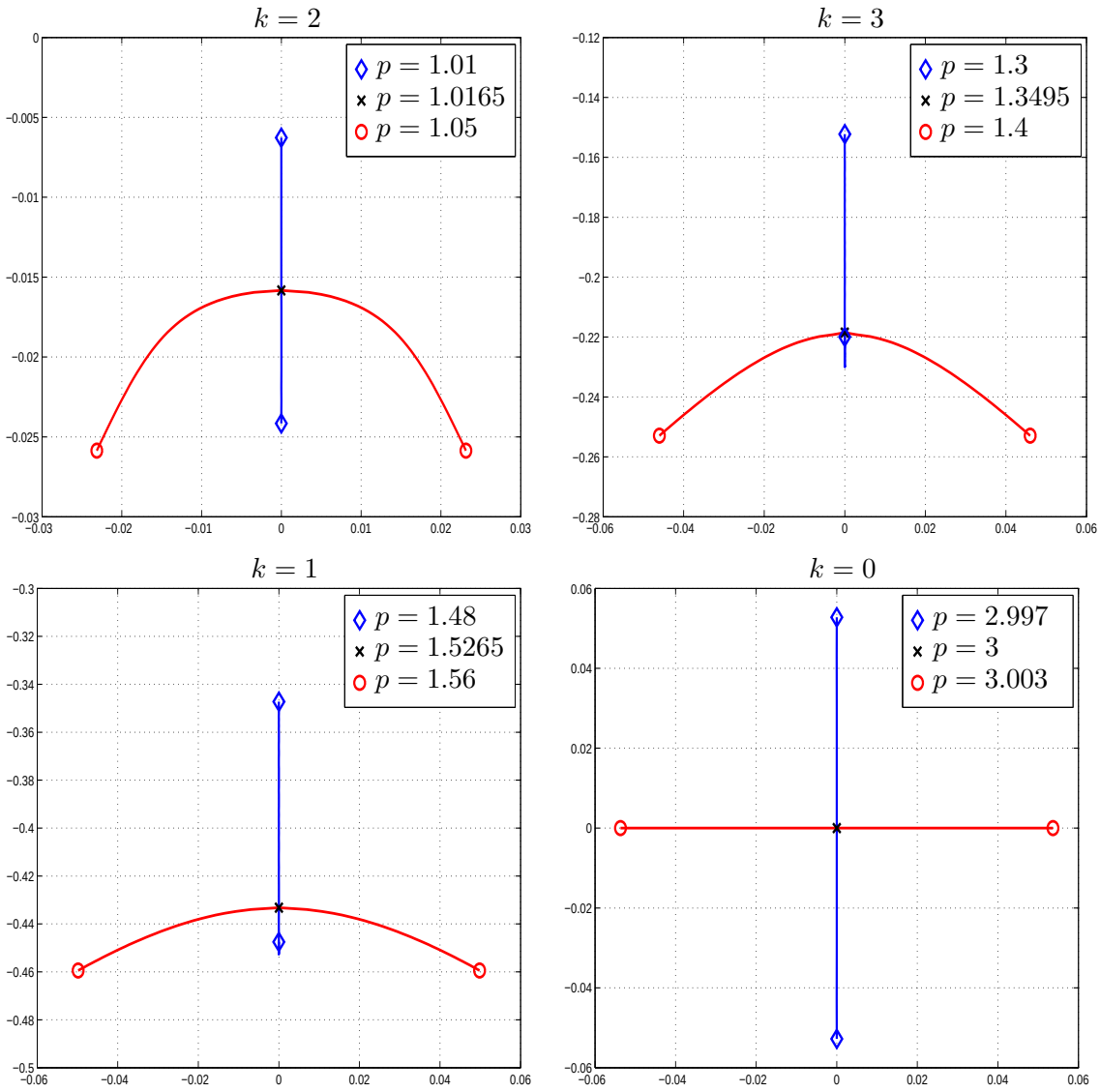

Figure 14: Bifurcation diagrams of $L_{m,k}$ for $m = 1$ and $0 \leq k \leq 3$.

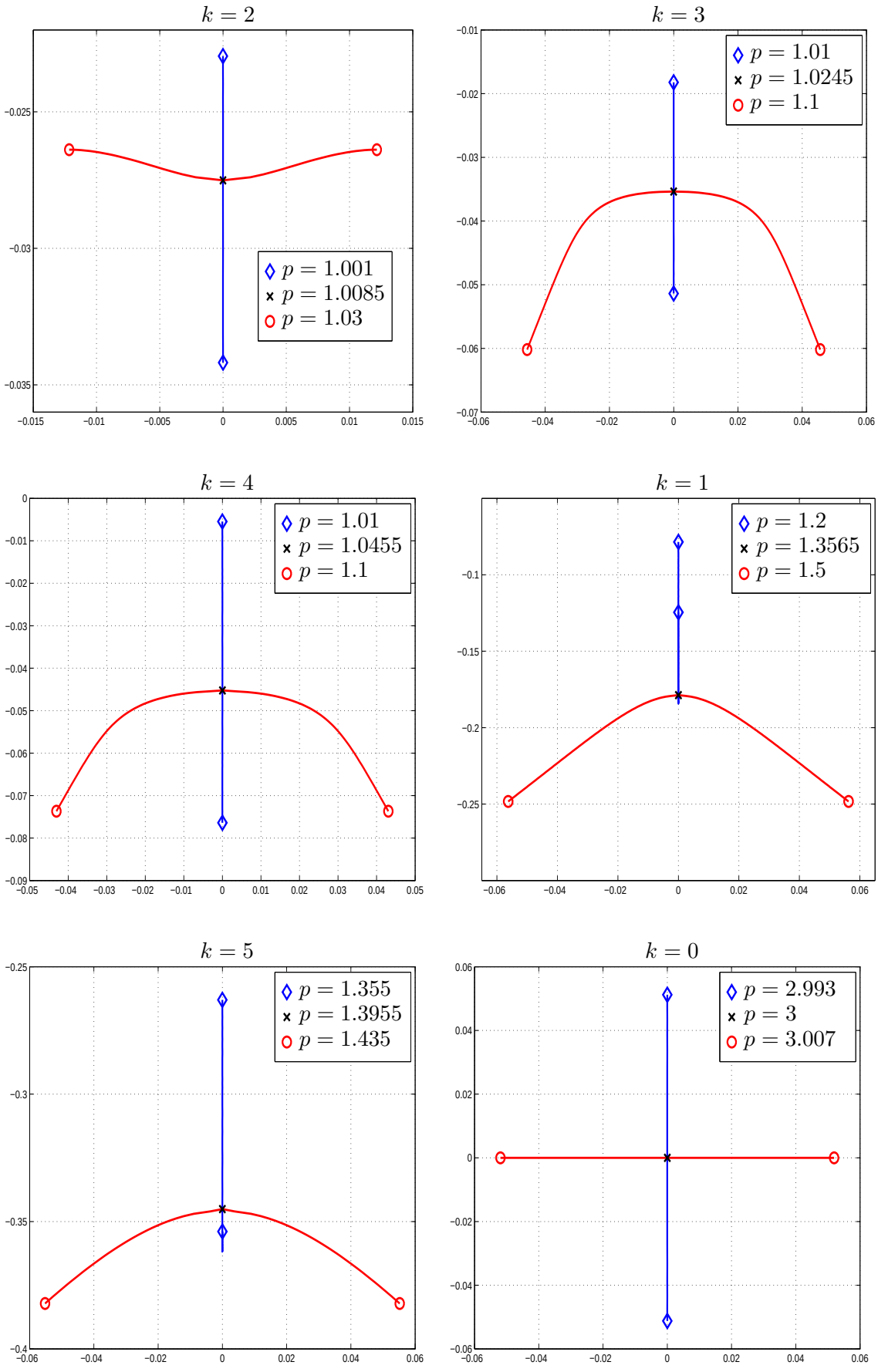

Figure 15: Bifurcation diagrams of $L_{m,k}$ for $m = 2$ and $0 \leq k \leq 5$.